RESEARCH PAPER

Non-THC cannabinoids inhibit prostate carcinoma growth *in vitro* and *in vivo*: pro-apoptotic effects and underlying mechanisms

Luciano De Petrocellis[1]*, Alessia Ligresti[2]*, Aniello Schiano Moriello[1], Mariagrazia Iappelli[1], Roberta Verde[2], Colin G Stott[3], Luigia Cristino[1], Pierangelo Orlando[4]* and Vincenzo Di Marzo[2]

[1]*Istituto di Cibernetica, Endocannabinoid Research Group, Consiglio Nazionale delle Ricerche, Pozzuoli, Italy,* [2]*Istituto di Chimica Biomolecolare, Endocannabinoid Research Group, Consiglio Nazionale delle Ricerche, Pozzuoli , Italy,* [3]*GW Pharma Ltd, Salisbury, UK, and* [4]*Istituto di Biochimica delle Proteine, Endocannabinoid Research Group, Consiglio Nazionale delle Ricerche, Napoli, Italy,*

Correspondence
Luciano De Petrocellis or Vincenzo Di Marzo, Endocannabinoid Research Group, Consiglio Nazionale delle Ricerche, Via Campi Flegrei 34, Comprensorio Olivetti, 80078, Pozzuoli (NA), Italy. E-mail: l.depetrocellis@cib.na.cnr.it or vdimarzo@icb.cnr.it

----

*These authors devoted equal experimental effort to this work

----

BACKGROUND AND PURPOSE

Cannabinoid receptor activation induces prostate carcinoma cell (PCC) apoptosis, but cannabinoids other than Δ^9-tetrahydrocannabinol (THC), which lack potency at cannabinoid receptors, have not been investigated. Some of these compounds antagonize transient receptor potential melastatin type-8 (TRPM8) channels, the expression of which is necessary for androgen receptor (AR)-dependent PCC survival.

EXPERIMENTAL APPROACH

We tested pure cannabinoids and extracts from *Cannabis* strains enriched in particular cannabinoids (BDS), on AR-positive (LNCaP and 22RV1) and -negative (DU-145 and PC-3) cells, by evaluating cell viability (MTT test), cell cycle arrest and apoptosis induction, by FACS scans, caspase 3/7 assays, DNA fragmentation and TUNEL, and size of xenograft tumours induced by LNCaP and DU-145 cells.

KEY RESULTS

Cannabidiol (CBD) significantly inhibited cell viability. Other compounds became effective in cells deprived of serum for 24 h. Several BDS were more potent than the pure compounds in the presence of serum. CBD-BDS (i.p.) potentiated the effects of bicalutamide and docetaxel against LNCaP and DU-145 xenograft tumours and, given alone, reduced LNCaP xenograft size. CBD (1–10 μM) induced apoptosis and induced markers of intrinsic apoptotic pathways (PUMA and CHOP expression and intracellular Ca^{2+}). In LNCaP cells, the pro-apoptotic effect of CBD was only partly due to TRPM8 antagonism and was accompanied by down-regulation of AR, p53 activation and elevation of reactive oxygen species. LNCaP cells differentiated to androgen-insensitive neuroendocrine-like cells were more sensitive to CBD-induced apoptosis.

CONCLUSIONS AND IMPLICATIONS

These data support the clinical testing of CBD against prostate carcinoma.

LINKED ARTICLE

This article is commented on by Pacher *et al.*, pp. 76–78 of this issue. To view this commentary visit http://dx.doi.org/10.1111/j.1476-5381.2012.02121.x

Abbreviations

AR, androgen receptor; BDS, botanical drug substance; BCL, binding component 3-BBC3; BRM, botanical raw material; CBC, cannabichromene; CBD, cannabidiol; CBDA, cannabidiolic acid; CBDV, cannabidivarin; CBG, cannabigerol; CBGA, cannabigerolic acid; CBGV, cannabigevarin; CBN, cannabinol; CHOP, CCAAT/enhancer binding protein or DDIT3, DNA-damage-inducible transcript 3; Cq, threshold cycles; ER, endoplasmic reticulum; ERα, oestrogen receptor 1;

ERβ, oestrogen receptor 2; GPER, G-protein-coupled oestrogen receptor 1; MTT, 3-(4,5-dimethylthiazol-2-yl)-2,5-diphenyltetrazolium bromide; NGF, nerve growth factor; NSE, neuron-specific enolase; OMDM233, phenyl-4-phenyl (–)-menthylamine; p21, cyclin-dependent kinase inhibitor 1A; p27^{Kip}, cyclin-dependent kinase inhibitor; p53, tumour protein; PCC, prostate carcinoma cell; PUMA, p53-up-regulated modulator of apoptosis; qRT-PCR, quantitative real-time-PCR; RNA pol, RNA polymerase II subunit; ROS, reactive oxygen species; SDP, serum deprivation; THC, Δ⁹-tetrahydrocannabinol; THCA, Δ⁹-tetrahydrocannabinolic acid; THCV, Δ⁹-tetrahydrocannabivarin; THCVA, Δ⁹-tetrahydrocannabivarinic acid; TRP, transient receptor potential channel; TRPA1, transient receptor potential cation channel, subfamily A, member 1; TRPM8, transient receptor potential cation channel, subfamily M, member 8; TRPV1, transient receptor potential cation channel, subfamily V, member 1; TRPV2, transient receptor potential cation channel, subfamily V, member 2; TTBS, TBS plus 0.5% Tween 20, pH 7.4

Introduction

The rapid progress of the research on cannabinoids has contributed to the understanding of the biological actions of these molecules and of their medical significance, which encompass a broad spectrum of physiological and pathological mechanisms in diverse cell types (Bab, 2011). Cannabinoids can be used for treatment of the nausea and vomiting associated with chemotherapy in cancer patients (Robson, 2005; Galal et al., 2009). There is also evidence that Δ⁹-tetrahydrocannabinol (THC) and synthetic agonists of cannabinoid CB₁ and CB₂ receptors, as well as endocannabinoids, are promising regulators of malignant cell growth (receptor and channel nomenclature follows Alexander et al., 2011). In most cases, these actions have been attributed to the ability of these compounds to activate the cannabinoid receptors or, (as in the case of anandamide) the transient receptor potential (TRP) vanilloid type-1 (TRPV1) channel (Munson et al., 1975; De Petrocellis et al., 1998; Maccarone et al., 2000; Bifulco et al., 2001; Jacobsson et al., 2001; Sanchez et al., 2001; Casanova et al., 2003; Ligresti et al., 2003; Mimeault et al., 2003; Contassot et al., 2004; Caffarel et al., 2010; Guindon and Hohmann, 2011). Cannabinoid receptor agonists, apart from their pro-apoptotic and anti-proliferative anticancer activities, may also affect tumour cell angiogenesis, migration, invasion, adhesion and metastasis (Blázquez et al., 2003; Portella et al., 2003; Preet et al., 2008).

Non-THC cannabinoids have also been tested in cancer (Izzo et al., 2009; Gertsch et al., 2010; Russo, 2011). Cannabidiol (CBD), which is very abundant in certain strains of *Cannabis*, has very low affinity for CB₁ and CB₂ receptors, and activates TRPV1 channels (Bisogno et al., 2001). This compound induces apoptosis in a triple-negative breast carcinoma cell line and inhibits tumour cell growth and metastasis (Ligresti et al., 2006; Ramer et al., 2010; McAllister et al., 2011; Aviello et al., 2012). CBD and other non-THC cannabinoids [i.e. cannabigerol (CBG), cannabichromene (CBC), cannabidiolic acid (CBDA) and Δ⁹-tetrahydrocannabidiolic acid (THCA)] have been assessed against a number of tumour cell lines distinct in origin and typology. These compounds have been compared with extracts [known as 'botanical drug substances', (BDS)] from corresponding *Cannabis* strains (Ligresti et al., 2006). Indeed, the testing of BDS enriched in a certain cannabinoid might demonstrate potentially important synergistic effects between cannabinoid and non-cannabinoid cannabis components, which, in turn might be useful therapeutically. The results obtained indicated that, of these five pure compounds and BDS tested, CBD and CBD–BDS were

usually the more effective inhibitors of cancer cell growth, with little or no activity on non-cancer cells (Ligresti et al., 2006). CBD inhibits also glioblastoma growth and potentiates the action of THC on this type of tumour (Torres et al., 2011). However, these effects are only marginally dependent upon interaction with cannabinoid and TRPV1 receptors (Massi et al., 2004; Vaccani et al., 2005; Torres et al., 2011).

Prostate carcinoma is a major life-threatening disease in men and WHO predicts that deaths from this type of cancer will double over the next 30 years (Bahnson, 2007; Jemal et al., 2009). Hence, novel therapeutic approaches are urgently required. Endocannabinoids, through interaction with CB₁ receptors and synthetic endocannabinoid-vanilloid hybrids via stimulation of TRPV1 channels have been shown to inhibit nerve growth factor (NGF)-induced proliferation of human prostate PC-3 cells (Melck et al., 2000). However, THC can induce apoptosis of these cells via a receptor-independent mechanism (Ruiz et al., 1999), but also increase the production of the pro-proliferative factor, NGF (Velasco et al., 2001). A role for CB₂ receptors in the induction of prostate carcinoma cell (PCC) apoptosis has been described (Sarfaraz et al., 2005; Olea-Herrero et al., 2009). On the other hand, the prototype TRPV1 agonist, capsaicin, produces both pro-proliferative and pro-apoptotic effects on PCCs (Sanchez et al., 2005; 2006; Czifra et al., 2009; Ziglioli et al., 2009; Malagarie-Cazenave et al., 2009; 2011) and not necessarily via TRPV1 activation, but depending on the sensitivity of the cells to androgen. Moreover, it has been suggested that other TRP channels play a role in PCC survival. TRP channels of melastatin-type 8 (TRPM8) are over-expressed in androgen-dependent PCC lines in a manner dependent on androgen receptor (AR) activation (Horoszewicz et al., 1983; Tsavaler et al., 2001; Henshall et al., 2003; Zhang and Barritt, 2004; Bidaux et al., 2005; 2007). In contrast, TRP channel of vanilloid type-2 (TRPV2) are down-regulated by AR, and their activation stimulates PCC migration (Monet et al., 2010). These findings are relevant to current investigations of the anti-tumour activity of non-THC cannabinoids, as many such compounds and the corresponding BDS antagonize TRPM8 channels and activate and subsequently desensitize TRPV2 and TRPV1 channels (Qin et al., 2008; De Petrocellis et al., 2008; 2011). Furthermore, most of these compounds are also able to inhibit endocannabinoid inactivation (De Petrocellis et al., 2011). Therefore, they might act as 'indirect' cannabinoid receptor agonists, similar to synthetic compounds previously found to inhibit PCC growth (Nomura et al., 2011).

In the current study we tested 12 pure cannabinoids and nearly all the corresponding BDS on PCC growth *in vitro* and

in vivo. We investigated the cellular and molecular mechanisms of the putative effects of these compounds using both AR-positive and -negative PCC lines, under different culturing conditions, in the presence or absence of currently used chemotherapeutic agents, and after differentiation into a more malignant phenotype. By employing pharmacological, molecular biology, cell biology and immunofluorescence techniques *in vitro*, as well as xenograft tumour and survival studies in athymic mice, we suggest that non-THC cannabinoids, and CBD in particular, (much like THC, but without the typical psychotropic effects of this compound) might provide the bases for the development of novel therapeutic strategies for the treatment of prostate carcinoma.

Methods

Cannbinoids and Cannabis extracts

CBC, CBD, CBG, CBN, CBDA, CBGA (cannabigerol acid), CBDV (cannabidivarin), CBGV (cannabigevarin), THC, THCA, THCV (Δ^9-tetrahydrocannabivarin), THCVA (Δ^9-tetrahydrocannabivarin acid) and the corresponding BDS [extracts prepared from *Cannabis sativa* L. botanical raw material (BRM)] were provided by GW Pharmaceuticals Ltd. (Salisbury, UK). The compounds were at least 95% pure. The amount of each principal cannabinoid in the corresponding BDS varied between 24.1 and 67.5 (% w/w of extract), depending upon the BDS tested. A description of the cannabinoid content of each BDS is provided in the Supporting information. The proportion of each major cannabinoid in the BDS was used to calculate the amount of the BDS necessary to obtain the equimolar amount of the corresponding pure cannabinoid in the various experiments. The chemical profile of minor cannabinoids present in each BDS was unique to each BDS, as was that of non-cannabinoid components. Thus, each BDS has a unique chemical profile ('chemical fingerprint').

Cell cultures

Human prostate epithelial PC-3, DU-145, 22RV1 and LNCaP cells were purchased from Deutsche Sammlung von Mikroorganismen und Zellkulturen GmbH (DSMZ, Braunschweig, Berlin, Germany) and were maintained at 37°C in a humidified atmosphere containing 5% CO_2. Cells were cultivated according to the information provided in each case by the supplier. DU-145 and LNCaP cells were cultivated in RPMI-1640 medium supplemented with 10% FBS, 100 U·mL^{-1} penicillin and 0.1 mg·mL^{-1} streptomycin. PC-3 cells were cultivated in 45% RPMI-1640 and 45% Ham's F12 medium supplemented with 10% FBS, 100 U·mL^{-1} penicillin and 0.1 mg·mL^{-1} streptomycin. 22RV1 cells were cultivated in 40% RPMI-1640 and 40% DMEM medium supplemented with 20% FBS, 100 U·mL^{-1} penicillin and 0.1 mg·mL^{-1} streptomycin. Low cell passages (between 5 and 20) were used in this study. PC-3 and DU-145 cells are androgen-independent; that is, they do not need androgen to grow nor is their growth affected by androgens. 22RV1 cells are androgen-independent/androgen-responsive; that is, androgens are not required for growth but stimulate growth. LNCaP cells are androgen-dependent; that is, they require androgens in the culture medium in order to grow (van Bokhoven *et al.*, 2003).

Quantitative RT-PCR analyses

Total RNA was extracted from cell pellets in 1.0 mL of Trizol® (Invitrogen) following the manufacturer's instructions, dissolved in RNA storage solution (Ambion, Life Technologies, Grand Island, NY, USA), UV-quantified by a Bio-Photometer® (Eppendorf, Hamburg, Germany) and stored at –80°C until use. RNA aliquots (5 μg) were digested by RNAse-free DNAse I (Ambion DNA-free™ kit) in a 20 μL final volume reaction mixture to remove residual contaminating genomic DNA. After DNAse digestion, concentration and purity of RNA samples were evaluated by the RNA-6000-Nano® microchip assay using a 2100 Bioanalyzer® equipped with a 2100 Expert Software® (Agilent, Santa Clara, CA, USA) following the manufacturer's instructions. For all samples tested, the RNA integrity number (R.I.N.) was greater than 7 (on a 0–10 scale); 1 μg of total RNA, as evaluated by the 2100 Bioanalyzer, was reverse-transcribed in cDNA and analysed as previously described (Grimaldi *et al.*, 2009). Optimized primers for SYBR-green analysis and optimum annealing temperatures were designed by the Allele-Id software version 7.0 (PREMIER Biosoft International, Palo Alto, CA, USA) and were synthesized (HPLC purification grade) by Eurofins MWG, Ebersberg, Germany. In the presence of splicing variants, all the sequences were aligned and the primers were designed in the homologous regions. Primer sequences are listed in Table S1. Relative gene expression calculation, corrected for PCR efficiency and normalized with respect to the reference gene (RNA polymerase II subunit, Acc Z27113), was performed by the IQ5 software, as previously described (Grimaldi *et al.*, 2009).

Western blots

Cell pellets were homogenized in cold lysis buffer containing: 50 mM HEPES (pH 7.4), 1% Triton X-100, 0.25% sodium hydroxycholate, 150 mM NaCl, 2 mM EDTA, 10% glycerol, 1 mM benzamidine, 1 mM PMSF, 1/100 stock dilutions of a protease inhibitory cocktail (Sigma-Aldrich, St Louis, MO, USA) and 10 μL of phosphatase inhibitors (Sigma-Aldrich). Protein extracts were quantified according to Bradford's method (Bio-Rad, Hercules, CA, USA). Samples were diluted 1:1 in Laemmli sample buffer containing 5% β-mercaptoethanol and denaturated at 95°C for 5 min; 50 μg of protein per lane was separated on a Criterion TGX-stain free pre-casted 4–20% SDS gel at 150 V. Proteins were blotted to a PVDF membrane at 100 V for 50 min in cold Tris–glycine buffer, 20% methanol, and the membrane was blocked in 1xTBS (Bio-Rad) containing 1% casein (Roche Diagnostic GmbH, Mannheim, Germany) over night at 4°C. The membrane was incubated for 1 h at room temperatures with rabbit polyclonal antibody to TRPM8 (GeneTex, Irvine, CA) diluted to 1/1000 in blocking solution or purified mouse anti-human p53 DO-1 (Becton and Dickinson Biosciences, Franklin Lakes, NJ, USA) or purified mouse anti-p53 (pS46) (BD Pharmingen), both diluted to 1/250. TRPM8 transfected HEK-253 cells (De Petrocellis *et al.*, 2008) and HeLa cells were used as positive control for TRPM8 and p53 respectively. The membrane was washed twice with TTBS (TBS plus 0.5% Tween 20, pH 7.4) and twice with blocking solution at room temperature for 10 min. Primary antibody was detected by a goat anti-rabbit or anti-mouse HRP-conjugated secondary antibodies (Bio-Rad) diluted to 1/2000 in blocking solution. After washing four times with TTBS and a final wash by TBS, bound second-

ary antibody was visualized by the chemiluminescent Immun-Star Western C kit. Chemiluminescence values were collected and processed as described for the caspase 3/7 assay. The membranes were stripped at room temperature for 15 min using CHEMICON re-blot plus strong antibody stripping solution (Millipore, Schwalbach, Germany) and re-probed with rabbit polyclonal antibody against β-actin (ENZO Life Sciences, Farmingdale, NY, USA) diluted to 1/500 in blocking solution.

3-(4,5-Dimethylthiazol-2-yl)-2,5-diphenyltetrazolium bromide (MTT) assay

Cells were seeded in presence of 10% FBS in six-well dishes with varying density depending on the cell line (from 6×10^4 to 1×10^5 cells per well) and submitted to different treatment protocols. When the treatments were conducted in presence of serum after adhesion, cells were treated with increased concentrations of compounds for 72 h (the presence of serum was maintained during the treatments). When the treatments were conducted in the absence of serum, after adhesion, cells were serum-deprived for 16 h and subsequently treated with increased concentrations of compounds for 24 h (the absence of serum was maintained during the treatments). When the treatments were conducted in a protein-deprived serum, FBS was protein-deprived by centrifugation at $3000 \times g$ in Centriplus 30 kDa centrifugal filter devices (Millipore, Milan, Italy), and cells were directly seeded in presence of the 10% protein-deprived serum and treated under those conditions with increased concentrations of compounds for 72 h. Cell viability was assessed by the MTT assay. The ability of cells to reduce MTT provided an indication of the mitochondrial integrity and activity and has been interpreted as a measure of cell viability. Absorbance at 620 nm was read on a GENius-Pro 96/384 Multifunction Microplate Reader (GENios-Pro, Tecan, Milan, Italy). All compounds were dissolved in DMSO or ethanol. Fresh stock solutions were prepared on the day of the experiment. The final concentration of solvent was less than 0.1% per well. Optical density values from vehicle-treated cells were defined as 100% of MTT-reducing activity and the effects were measured as a % of the inhibition of the measures obtained with vehicle alone. When several concentrations of compounds or BDS were tested, data are reported as means $\pm$ SD of IC_{50} values calculated from three independent experiments. Statistical differences between groups were assessed by ANOVA followed by Bonferroni's test using GraphPad Software, La Jolla, CA, USA.

Measurement of caspase 3/7 activity

Apoptosis was evaluated by means of the Caspase-Glo® 3/7 Chemioluminescent Assay Kit (Promega Corporation, Madison, WI, USA) following the manufacturer's protocol. Human prostate carcinoma DU145, LNCaP, PC-3 and 22RV1 cells were cultured in the presence of drugs in different conditions for the times indicated. After incubation, cells were trypsinized as needed, washed with PBS and processed. The assay was performed in 96-well white-walled plates, adding 100 µL of Caspase-Glo® 3/7 reagent to each well containing 1×10^4 and 2×10^4 cells in 100 µL of culture medium. After 1 h incubation in the dark at room temperature, luminescence was measured by a VersaDoc MP System equipped by the Quantity One® version 4.6 software (Bio-Rad). All

samples were assayed at least in triplicate. Luminescence values from the blank reaction (vehicle-treated cells) were subtracted from experimental values. In order to evaluate the commitment to apoptosis of PCCs, cells grown in presence of vehicle were treated for 24 h with $0.1\ \mu g \cdot mL^{-1}$ S-(+)-camptothecin (Sigma-Aldrich) plus $0.2\ \mu g \cdot mL^{-1}$ anti Fas-antibody (Roche Diagnostic GmbH), two compounds known to potently induce apoptosis. Statistical analysis was performed by analysis of variance at each point using ANOVA followed by Bonferroni's test.

DNA fragmentation analyses

Analysis of DNA fragmentation was performed essentially as described in the Agilent tech-note number 5988-8028EN. Briefly, cell pellets containing about 2×10^6 cells were gently re-suspended at 4°C in 100 µL of lysis solution (0.2% Triton X-100, 10 mM Tris pH 8, 10 mM EDTA) and incubated for 5 min. After centrifugation at $13\ 000 \times g$ the supernatants were purified by a QIAquick PCR purification kit (QIAGEN, Hilden, Germany) (elution volume: 30 µL); 1 µL from each samples was run in a Agilent 2100 Bioanalyzer with the DNA 7500 Lab Chip kit (Agilent), following the manufacturer's instruction.

FACS scan analyses

1 mL of 70% ethanol at 4°C was added dropwise to the cell pellets whilst mixing gently . After incubation for 30 min, ethanol was discarded, and the cells were washed twice with 1 mL of PBS and then centrifuged at $400 \times g$ for 5 min. Pellets were re-suspended in 250 µL of PBS containing RNAse A-DNAsi free ($100\ \mu g \cdot mL^{-1}$) and incubated at 37°C for 30 min. Propidium iodide was added at final concentration of $20\ \mu g \cdot mL^{-1}$, and incubation (starting from 30 min to 2 h) was performed in the dark on ice until flow cytometry analysis. FACS analysis was performed to FACS-facility service of IGB-IBP of CNR-Naples, Italy by using a Becton-Dickinson FACS model CantoR. Statistical analysis was performed by the program ModFit LT version 3.0 (Verity Software House, Topsham, ME, USA).

TUNEL assays using a bioanalyser

The 'In situ cell death Detection kit, Fluorescein' kit (Roche Diagnostic GmbH) was used for these analyses After incubation with the compounds, cells were collected into 15 mL tubes (Falcon, Becton and Dickinson Biosciences) and washed twice with PBS and centrifuged at $250 \times g$ for 5 min at room temperature. The pellet was re-suspended in the fixative solution (4% paraformaldehyde) and incubated for 1 h with agitation. After two washes with PBS, to remove all the paraformaldehyde, the cells were incubated for 2 min in the permeabilization solution (0.1% TritonX-100, 0.1% sodium citrate) on ice. After two washes, the pellet obtained was re-suspended in 100 µL of the TUNEL reaction mixture (400 µL labelling solution plus 100 µL of the enzyme solution) and incubated (37°C) for 1 h in humidified atmosphere in the dark. Then cells were washed, re-suspended in 250 µL of 70% ethanol and treated with $20\ \mu g \cdot mL^{-1}$ of propidium iodide; and the suspension was incubated for 30 min on ice in the dark. The cells were then re-suspended in Cell Buffer (Agilent Technologies). Fluorescence was evaluated using a Bioanalyzer equipped with 2100 Expert Software (Agilent Technologies).

TUNEL and TRPM8 immunofluorescence measurements

LNCaP and DU-145 cells attached on slides (Deckglaser, 21 × 26 mm) in six-well culture plates, after CBD treatment or after serum deprivation, were used for TRPM8 and TUNEL double staining or TRPM8/calnexin double immunoreaction. After removal of cell culture media and three brief and delicate rinses in PBS, the cells were fixed in paraformaldehyde solution (4% in phosphate buffer with agitation at 4°C) for 20 min and then washed twice in PBS. For TRPM8 immunohistochemistry and TUNEL double staining, the cells were incubated overnight at +4°C with primary rabbit polyclonal anti-TRPM8 antibody (GeneTex) diluted to 1:400 in PBS (pH 7.4, 0.1 M) and then incubated for 4 h at +4°C with donkey anti-rabbit secondary antibody Alexa-Fluor 546 diluted to 1:200 in PBS. After rinsing in PBS, the same cells were processed for the TUNEL assay performed (see above) in accordance with the manufacturer's instructions. After 60 min incubation at 37°C in the dark and humidified atmosphere, the cells were rinsed in PBS and embedded with antifade before mounting on coverslips. Negative control for the TUNEL reaction was performed by incubation of CBD-treated LNCaP cells with labelling solution without the enzyme. No signal was observed after this treatment.

In order to provide evidence for the localization of TRPM8 channels in the endoplasmic reticulum, the TRPM8/calnexin double immunoreaction was performed in LNCaP cells after 30 min permeabilization in 0.1% Triton X-100 phosphate buffer solution and overnight incubation at 4°C in a mixture of anti-rabbit TRPM8 (GeneTex) and anti-goat calnexin (Santa Cruz Biotechnology, Santa Cruz, CA) primary antibodies, both diluted to 1:400 in 0.1% Triton X-100 phosphate buffer solution. Subsequently, the cells were rinsed in PBS and reacted for 4 h at +4°C with a mixture of donkey anti-goat Alexa 546 and donkey anti-rabbit Alexa 488, both diluted to 1:200 in 0.1% Triton X-100 phosphate buffer solution. Nuclear counterstaining with DAPI was performed before mounting the slices. Immunocytochemical TRPM8-negative control included pre-absorption of diluted anti-TRPM8 antibody with immunizing peptide or omission of either TRPM8 and Calnexin primary anti-sera. These experiments did not show any immunostaining. All the samples were examined with a fluorescence microscope (Leica DMI6000B) equipped with objective at differential interference contrast, appropriate filters and deconvolution system. Images were acquired by using the digital camera (Leica DFC420 connected to the microscope and the image analysis software Leica MM AF Analysis Offline for Z-stack acquisition (Leica, Germany).

Intracellular calcium and reactive oxygen species (ROS) assays

Prostate cells were grown on 100 mm diameter Petri dishes as described and maintained in 5% CO_2 at 37°C. On the day of the experiment, the cells were loaded for 1 h at 25°C with the selective cytoplasmic calcium indicator Fluo-4AM (Invitrogen, Life Technologies, Grand Island, NY, USA), 4 μM in DMSO containing 0.02% Pluronic F-127 (Invitrogen). After loading, cells were washed twice in Tyrode's buffer (145 mM NaCl, 2.5 mM KCl, 1.5 mM $CaCl_2$, 1.2 mM $MgCl_2$, 10 mM D-glucose and 10 mM HEPES, pH 7.4), re-suspended in the same buffer and transferred to the quartz cuvette of the spectrofluorimeter (λ_{EX} = 488 nm, λ_{EM} = 516 nm) (Perkin-Elmer LS50B equipped with PTP-1 Fluorescence Peltier System; Perkin-Elmer Life and Analytical Sciences, Waltham, MA) under continuous stirring. Experiments were carried out by measuring cell fluorescence at 25°C before and after the addition of various concentrations of the test compounds. Agonist activity was determined in comparison with the maximum increase of intracellular Ca^{2+} due to the application of 4 μM ionomycin (Alexis Biochemicals, Lausen, Switzerland) and EC_{50} values were determined. In some experiments, cells were loaded with Fura-2-AM (2.5 μM) in Ca^{2+}-free buffer solution containing $MgCl_2$ in amounts equivalent to $CaCl_2$ and 0.1 mM EGTA. The dye was excited at 340 and 380 nm to monitor relative $[Ca^{2+}]i$ changes by the F_{340}/F_{380} ratio, and the emission was at 540 nm. Changes in fluorescence were monitored after a 5 min stabilization period, in a 0–300 s time interval after cell stimulation. All determinations were performed at least in triplicate. Curve fitting (sigmoidal dose–response variable slope) and parameter estimation were performed with GraphPad Prism® (GraphPad Software Inc., San Diego, CA). Statistical analysis of the data was performed at each point using ANOVA followed by Bonferroni's test.

Intracellular ROS generation was determined by spectrofluorometric analysis. PCCs were plated (1 × 10⁶ cells per Petri dish) for 24 h. On the day of the experiment, cells were rinsed once with Tyrode's buffer then loaded (1 h at 37°C in darkness) with 10 μM 2′,7′-dichlorofluorescein diacetate (fluorescent probe; Molecular Probes, Eugene, OR). Reactive ROS-induced fluorescence of intracellular 2′,7′-dichlorofluorescein diacetate was measured with a microplate reader (PerkinElmer LS50B, λ_{Ex} = 495 nm; λ_{Em} = 521 nm). Fluorescence was measured after incubation with 100 μM H_2O_2 and/or increasing concentrations of cannabinoids at room temperature in the darkness for different times (0–30–60–120 min). The fluorescence measured at time 0 was considered as basal ROS production and subtracted from the fluorescence at different times (Δ_1). Data are reported as mean ± SEM of Δ_2 (i.e. fluorescence Δ_1 values at different doses minus the Δ_1 values of cells incubated with vehicle). In some experiments, a buffer containing $MgCl_2$ in amounts equivalent to $CaCl_2$ and 0.1 mM EGTA and cells preloaded for 30 min with BAPTA-AM (40 μM) were used instead.

In vivo xenograft assays of anti-tumour activity

All animal care and experimental procedures complied with the Home Office Project Licence. All studies involving animals are reported in accordance with the ARRIVE guidelines for reporting experiments involving animals (McGrath et al., 2010). These tests were performed at PRECOS, UK, by Dr David Kendall, whose valuable help is acknowledged. Male MF-1 nude mice aged 4–7 weeks old (supplier: Harlan, Shardlow, UK; total 180) were used for the study. Mice were maintained in sterile isolators within a barriered unit illuminated by fluorescent lights set to give a 12 h light–dark cycle (on 07:00, off 19:00). The room was air-conditioned by a system designed to maintain an air temperature range of 23 ± 2°C. Mice were housed in social groups of five during the procedure in plastic cages (Techniplast, Kettering, UK) with irradiated bedding and provided with both nesting materials

and environmental enrichment. Mice were fed on sterile irradiated 2019 rodent diet (Harlan Teckland, UK) and autoclaved water was offered *ad libitum*. Animal welfare was checked daily. Each animal was allocated a unique identification number by implantation of a transponder.

There were six experimental groups for each cell line studied (LNCaP and DU-145 cells), with 10 mice per group; the groups consisted of the following:

Group 1 Vehicle
Group 2 1 mg·kg^{-1} CBD-BDS i.p. daily.
Group 3 10 mg·kg^{-1} CBD-BDS i.p. daily
Group 4 100 mg·kg^{-1} CBD-BDS i.p. daily
Group 5 either 5 mg·kg^{-1} docetaxel, i.v. once weekly, or 25–50 mg·kg^{-1} bicalutamide, p.o. three times per week
Group 6 100 mg·kg^{-1} CBD-BDS i.p. daily plus either 5 mg·kg^{-1} docetaxel, i.v. once weekly, or 25–50 mg·kg^{-1} bicalutamide p.o. three times per week

For the LNCaP xenograft studies, LNCaP cells were maintained *in vitro* in RPMI culture medium (Sigma, Poole, UK) containing 10% (v/v) heat-inactivated FBS (Sigma), 2 mM L-glutamine (Sigma) at 370C in 5% CO_2 and humidified conditions. Cells from sub-confluent monolayers were harvested with 0.025% EDTA, washed in culture medium and re-suspended in Matrigel for *in vivo* administration at 1–2×10^7 cells in 200 μL and were injected s.c. into the left flank of mice. The mice were anaesthetized and a pellet of 5-α-dihydrotestosterone (0.5 mg; 21 day release; Innovative Research of America, Sarasota, FL, USA) was implanted s.c. into the scruff of each mouse to facilitate the initial xenograft implant and growth. The wound was closed with Michel clips.

For the CBD-BDS DU145 cell study, the cells were maintained *in vitro* in RPMI culture medium (Sigma) containing 10% (v/v) heat-inactivated FBS (Gibco, Paisley, UK) at 37°C in 5% CO_2 and humidified conditions. Cells from sub-confluent monolayers were harvested with 0.025% EDTA, washed in culture medium and re-suspended in Matrigel for *in vivo* administration at 5×10^5 cells in 200 μL and were injected s.c. into the left flank of mice. Tumour dimensions were recorded at day 7 (calliper measurement of length and width and tumour cross-sectional area and volume calculated) and were recorded three times weekly, and body weight was measured weekly. When the tumour volume reached between 100 and 200 mm^3 (2–3 weeks), mice were allocated to their treatment groups. Mice were evaluated daily by an experienced technician for 4–5 weeks. CBD–BDS was formulated in 1:1:18 ethanol : Cremophor : 0.9% saline as follows: CBD–BDS was weighed into a glass vial and dissolved in ethanol to 20× final concentration and vortexed. CBD–BDS was prepared daily from ethanol stocks stored at –20°C. An equal volume of Cremophor was added and vortexed. Finally, 18 times the volume of saline was added to the solution and vortexed. Compounds were prepared on a weekly basis and stored at 4°C. The final concentration of the dosing solutions was determined according to the mean weight of the mice in each group at the start of the study and weekly thereafter. Each animal remained in the study until terminated, or until removal of that mouse from the study. Animals were removed at any time during the study if the tumour size became

excessive or any adverse effects were noted (complying with the UK Home Office Project Licence). At termination, the mice were anaesthetized (with Hypnorm, Janssen and Hynovel, Roche; equivalent to 4.5mg kg^{-1} fentanyl, 14.3mg kg^{-1} fluanisone and 7.1mg kg^{-1} midazolam) and blood was removed by cardiac puncture, processed for plasma and frozen at –20°C. The mice were then killed by decapitation. Tumours were excised, weighed, half-fixed in formalin and embedded into paraffin, half frozen and stored at –20°C. For the first CBD-BDS bicalutamide LNCaP study, dosing was initiated on day 15, and the study was terminated on day 38. For the second CBD-BDS bicalutamide LNCaP studies, mice were killed in a staggered manner when tumour volume exceeded 1700 mm^3, and data are presented as a survival plot.

Materials

Bicalutamide, docetaxel, testosterone and 17β-oestradiol were from Sigma-Aldrich (St. Louis, MO); CB receptor antagonists and agonists were supplied by Cayman Chemicals (Ann Arbor,MI) and TRP channel agonists and blockers and G15 by Tocris Bioscience (Bristol, UK).

Results

Expression of TRP channels in PCC lines under various experimental conditions

As shown by quantitative-real time PCR analyses, all four cell lines expressed at least one of the four TRP channels investigated, under all culturing conditions (Figure S1A and data not shown). All PCCs, except LNCaP cells, expressed TRPV1 and TRPA1 channels. TRPV2 was expressed in DU-145 and PC-3 cells only. LNCaP cells and, to a smaller extent, PC-3 cells expressed only the short variant of TRPM8 channels, the mRNA of which, in the former cells, was down-regulated following serum deprivation (see below). Addition of testosterone (50 μM) partly reversed TRPM8 down-regulation, a result which is in agreement with previous literature (Zhang and Barritt, 2004; Bidaux *et al.*, 2005) (see below). However, contrary to previous reports (Monet *et al.*, 2010) no up-regulation of TRPV2 channels was observed, even after prolonged serum deprivation in LNCaP cells (data not shown). Although TRPM8 mRNA was already reduced by a 24 h serum deprivation (see below), the TRPM8 protein was not, as shown by Western blot (Figure S1C) and immunocytofluorescence analyses (see below). Finally, CB$_1$ and CB$_2$ receptors were abundantly expressed in PC-3 cells, much less so in LNCaP cells, whilst DU-145 cells expressed some CB$_2$ mRNA and 22RV1 cells some CB$_1$ mRNA (Figure S1B).

Effect of cannabinoid receptor or TRP channel agonists and antagonists on PCC viability in MTT assays

We tested well-established agonists and antagonists of TRP channel and cannabinoid receptors in LNCaP and DU-145 cells using the MTT assay (Figure S2). Relatively low concentrations of capsaicin, but not resiniferatoxin, evoked a small, albeit significant, stimulatory effect on the viability of both cell lines (Figure S2A). Only very high and likely non-

Table 1

Effect of plant cannabinoids on the viability of human prostate carcinoma androgen receptor-negative (DU-145) cells

Pure compound	IC$_{50}$ (µM) on cell viability [A]	IC$_{50}$ (µM) on cell viability [B]	BDS	IC$_{50}$ (µM) on cell viability [A]	IC$_{50}$ (µM) on cell viability [B]
CBD	25.3 ± 8	5.4 ± 1	CBD BDS	9.0 ± 4	7.8 ± 2
CBC	>25 (40.7%)	8.5 ± 3	CBC BDS	9.2 ± 3	7.9 ± 1
CBG	>25 (17.3%)	10.4 ± 1	CBG BDS	10.4 ± 5	6.9 ± 2
CBDV	21.0 ± 4	20.0 ± 5	CBDV BDS	17.1 ± 7	10.3 ± 1
THCV	>25 (38.6%)	20.5 ± 3	THCV BDS	>25 (41.0%)	8.3 ± 1
THCVA	>25 (25.6%)	>25 (36.1%)	THCVA BDS	>25 (30.9%)	12.4 ± 1
THCA	>25 (21.9%)	21.6 ± 2	THCA BDS	18.9 ± 2	9.9 ± 2
CBDA	>25 (11.2%)	10.9 ± 4	CBDA BDS	>25 (27.8%)	15.9 ± 2
CBGA	>25 (7.7%)	11.2 ± 2	CBGA BDS	19.2 ± 2	12.3 ± 3
CBGV	>25 (11.3%)	>25 (23.3%)	CBGV BDS	>25 (21.9%)	10.2 ± 2
CBN	>25 (17.2%)	>25 (21.8%)	–	–	–
THC	>25 (6.6%)	11.7 ± 3	–	–	–

(A) Cells were seeded in presence of 10% FBS in six-well Multiwell with a density of 8×10^4 cells·per well. After adhesion, cells were treated with increasing concentrations of compounds for 72 h (presence of serum was maintained during the treatments). (B) Cells were seeded in presence of 10% FBS in six-well Multiwell with a density of 8×10^4 cells·per well. After adhesion, cells were starved for 16 h and subsequently treated with increasing concentrations of compounds for 24 h (absence of serum was maintained during the treatments). Cell viability was assessed by MTT staining. Data are reported as mean ± SD of IC$_{50}$ values calculated from three independent experiments. In the case of IC$_{50}$ > 25 µM, the maximum inhibition observed at the highest concentration tested (25 µM) is shown.

selective doses of capsaicin, and much less so resiniferatoxin, inhibited cell viability, and these effects were not antagonized by the selective TRPV1 antagonist, iodo-resiniferatoxin (data not shown). Allylisothiocyanate, a TRPA1 agonist, inhibited cell viability, but this effect was not reversed by two different TRPA1 antagonists, HC030031 and AP18 (Figure S2B). Finally, icilin, a synthetic TRPM8 agonist, evoked a small, albeit significant, stimulatory effect on the viability of LNCaP, but not DU-145, cells; whereas phenyl-4-phenyl (–)-menthylamine (OMDM233), a selective TRPM8 channel antagonist (Ortar et al., 2010), inhibited LNCaP, but not DU-145, cell viability (Figure S2C). The effect of this compound reached a plateau of 25–30% inhibition at 1 µM (which is much higher than IC$_{50}$ at rat recombinant TRPM8 channels (Ortar et al., 2010), and higher concentrations did not cause greater inhibition. A strong inhibitory effect of dual CB$_1$/CB$_2$ receptor agonists (HU210, WIN55,212-2) was observed on both DU-145 and LNCaP cells, but only at concentrations (>5 µM) incompatible with their K_i at cannabinoid receptors (Figure S2D). This effect was not antagonized by the selective CB$_1$ antagonist SR141716 (0.5 µM) or the selective CB$_2$ antagonist SR144528 (0.5 µM), (Figure S2D). Studies in other cancer cells (human colorectal carcinoma Caco-2 cells) have shown effects of synthetic and endogenous cannabinoids on viability via mechanisms not involving cannabinoid receptors (see Gustafsson et al., 2009 for an example). The CB$_1$ receptor-selective agonist arachidonyl-2-chloroethylamide and the CB$_2$ receptor-selective agonist JWH133, did not exhibit any significant effect on the two cell lines at concentrations up to 10 µM (not shown). Finally, a selective endocannabinoid uptake inhibitor (OMDM-1) inhibited cell viability only at concentrations >10 µM (max inhibition 51.6%; data not

shown). This concentration is higher than its reported IC$_{50}$ against anandamide cellular reuptake (Ortar et al., 2003). In PC-3 cells, which exhibit the highest expression levels of CB$_1$ and CB$_2$ receptors (see above), HU210 and WIN55,212-2 only inhibited cell viability at concentrations ≥5 µM (data not shown).

Effect of cannabinoids and BDS on PCC viability in MTT assays

For these experiments, all PCC lines were used. In particular, the complete panel of cannabinoids and relative BDS were screened in DU-145 and LNCaP in the presence and/or absence of serum, whereas only the pure compounds were screened in 22RV1 and PC-3 cells under these two conditions. As shown in Tables 1 and 2, of all non-THC cannabinoids tested in DU-145 and LNCaP cells, CBD was among the most potent inhibitors of cell viability, followed by CBC, in presence of serum. The corresponding BDS were usually as potent and efficacious as the pure compounds, and in many cases their effects were stronger in the presence of serum. However, a 'cannabinoid-free' BDS, obtained by eliminating CBG from CBG–BDS (De Petrocellis et al., 2011), and tested in amounts corresponding to those present in 10 µM of CBG–BDS, was nearly inactive in both DU-145 and LNCaP cells (15 ± 5% and 26 ± 18% inhibition, respectively, means ± SEM, N = 3). Importantly, and in full agreement with previous observations in glioma cells (Jacobsson et al., 2000), in both cell lines, pure cannabinoids and BDS became potent and efficacious at inhibiting the viability of cells previously kept for 15 h without serum and with an additional 24 h incubation without serum. Similar results were obtained in PC-3 and 22RV1 cells (Tables S2 and S3).

Table 2

Effect of plant cannabinoids on the viability of human prostate carcinoma androgen receptor-positive (LNCaP) cells

Pure compound	IC$_{50}$ (μM) on cell viability [A]	IC$_{50}$ (μM) on cell viability [B]	BDS	IC$_{50}$ (μM) on cell viability [A]	IC$_{50}$ (μM) on cell viability [B]
CBD	25.0 ± 3	5.7 ± 2	CBD BDS	18.1 ± 6	6.6 ± 2
CBC	20.0 ± 5	10.9 ± 3	CBC BDS	>25 (25.6%)	7.9 ± 1
CBG	>25 (34.5%)	11.2 ± 4	CBG BDS	21 ± 8	9.0 ± 1
CBDV	>25 (27.6%)	20.0 ± 3	CBDV BDS	>25 (24.4%)	10.4 ± 1
THCV	>25 (28.5%)	17.5 ± 3	THCV BDS	16.3 ± 5	7.2 ± 1
THCVA	>25 (32.4%)	11.5 ± 5	THCVA BDS	19.4 ± 8	5.6 ± 1
THCA	22.1 ± 2	17.1 ± 1	THCA BDS	15.0 ± 2	4.0 ± 3
CBDA	>25 (30.2%)	16.2 ± 5	CBDA BDS	>25 (34.5%)	9.3 ± 2
CBGA	>25 (7.0%)	11.6 ± 2	CBGA BDS	14.5 ± 2	8.5 ± 2
CBGV	>25 (23.9%)	>25 (41.0%)	CBGV BDS	>25 (40.2%)	9.4 ± 2
CBN	14.5 ± 6	>25 (34.2%)	–	–	–
THC	16.9 ± 3	5.5 ± 3	–	–	–

(A) Cells were seeded in presence of 10% FBS in six-well Multiwell with a density of 1×10^5 cells·per well. After adhesion, cells were treated with increasing concentrations of compounds for 72 h (presence of serum was maintained during the treatments). (B) Cells were seeded in presence of 10% FBS in six-well Multiwell with a density of 1×10^5 cells·per well. After adhesion, cells were starved for 16 h and subsequently treated with increasing concentrations of compounds for 24 h (absence of serum was maintained during the treatments). Cell viability was assessed by MTT staining. Data are reported as mean ± SD of IC$_{50}$ values calculated from three independent experiments. In the case of IC$_{50}$ > 25 μM, the maximum inhibition observed at the highest concentration tested (25 μM) is shown.

These data suggest that the presence of serum during the MTT assay might counteract the inhibitory effect of the compounds on PCC viability, and so we next examined in detail whether the addition of BSA to serum-deprived media would reduce the inhibitory effects of CBD, CBG and CBC (Figure 1A). We also compared the effects of the high potency compounds in cells cultured under conditions of serum deprivation and in protein-deprived sera (see Methods) (Figure 1B). The compounds exhibited good efficacy and potency at inhibiting cell viability in both cell lines only if high molecular weight proteins were absent from the serum. In contrast, the addition of testosterone or 17β-oestradiol in a serum-deprived medium did not significantly modify the effect of CBD (Figure 1C).

We finally tested if various antagonists of cannabinoid receptors (SR141716 or SR144528, 0.5 μM), TRPV1 (iodo-resiniferatoxin, 1 μM) and TRPA1 (HC030031 and AP18, 30 μM) channels, or an agonist of TRPM8 channels (icilin, 2 μM), influenced the inhibitory effects of CBD in the MTT assays under serum-deprived conditions, and found no significant effect with any of these compounds (data not shown).

Interactions between the effect of CBD and bicalutamide or docetaxel on PCC viability in MTT assays

Two standard drugs for the treatment of prostate cancer, bicalutamide and docetaxel, were tested on either LNCaP or DU-145 cells, cultured in the presence of serum, with or without different concentrations of CBD. Given alone, docetaxel did not markedly affect the proliferation of LNCaP

cells (IC$_{50}$ > 25 μM), however, when tested in combination with pure CBD, a greater effect was observed, even though this appeared to be due to an additive effect (Figure S3A). Docetaxel was more effective at inhibiting DU-145 cell growth, and CBD (only at the lowest concentration tested) potentiated the effect of this compound (Figure S3C). Finally, CBD significantly enhanced the efficacy of bicalutamide (10 μM) on LNCaP cells, although only at the highest dose tested (Figure S3B).

Effect of a CBD-enriched Cannabis extract on xenograft tumour growth in vivo

We carried out studies *in vivo* on the effects of docetaxel, bicalutamide and CBD–BDS on xenograft tumours obtained in athymic mice with LNCaP and DU-145 cells. CBD–BDS dose-dependently inhibited the growth of xenografts from LNCaP, but not DU-145, cells. At the highest dose tested (100 mg·kg^{-1}, i.p.), the extract exerted an effect on LNCaP xenografts, quantitatively similar to that of docetaxel (5 mg·kg^{-1}, i.v.), although it reduced the tumour growth inhibitory effect of this agent (Figure 2A). In DU-145 cell xenografts, CBD–BDS significantly potentiated docetaxel (Figure 2B). In a second experiment with xenograft tumours from LNCaP cells, two doses (25 and 50 mg·kg^{-1}, p.o.) of bicalutamide alone or CBD–BDS alone (100 mg·kg^{-1}, i.p.) produced little effect on tumour weight and volume at the end of the treatment, possibly because this experiment was interrupted after only 35 days. However, co-administration of bicalutamide at 25 mg·kg^{-1} and CBD–BDS significantly inhibited xenograft growth (Figure 2C). In a third experiment, survival was assessed by Kaplan–Meier analysis. After
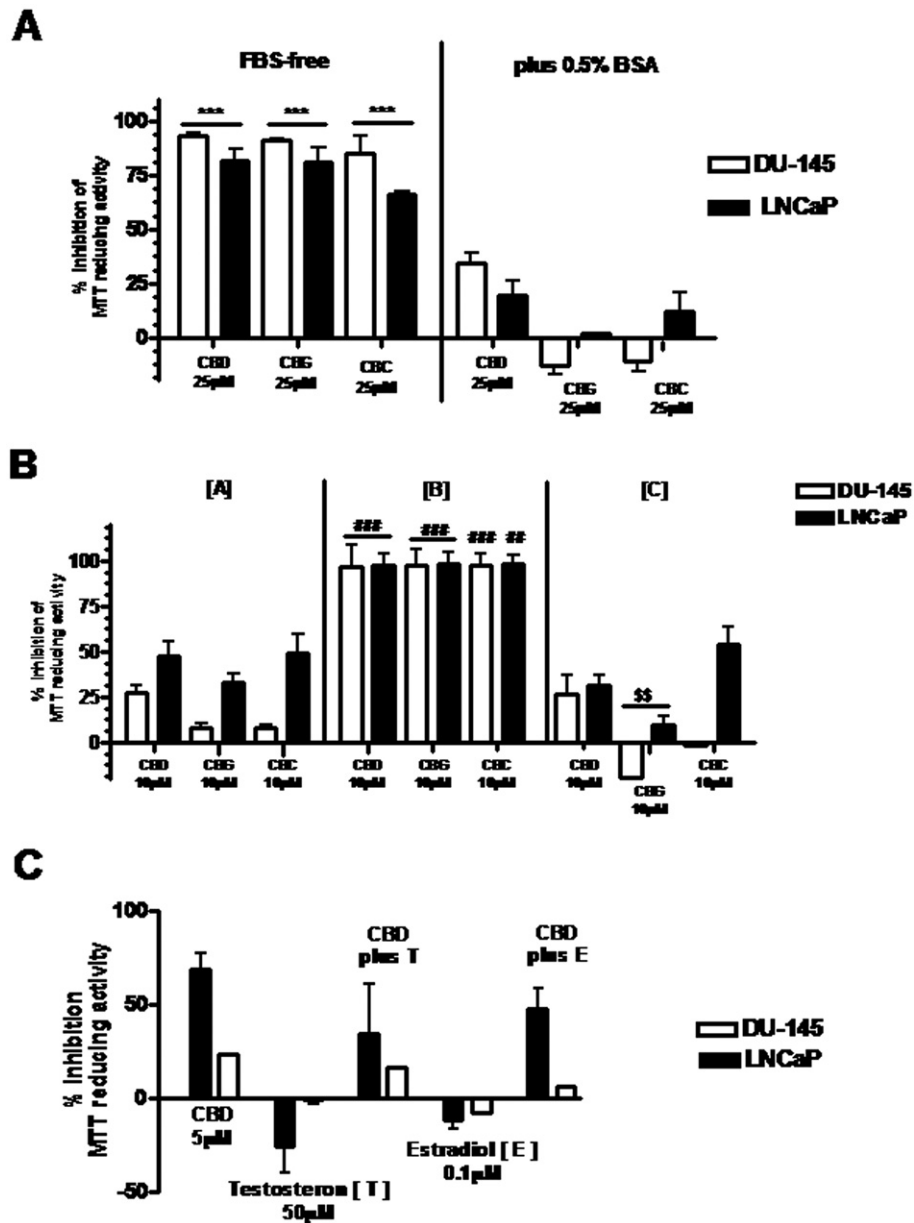
BJP

Figure 1

Serum deprivation or modification of serum content differently affects the effect of cannabinoids (CBD, CBG, CBC) on the viability of human PCCs in the MTT assay. (A) Cells were grown in presence of 10% FBS in six-well dishes. After adhesion, cells were serum-deprived (with or without 0.5%BSA) for 16 h and subsequently treated with compounds for 24 h. Cell viability was assessed by the MTT assay. Data shown are means $\pm$ SEM of % inhibition of MTT-reducing activity, calculated from three independent experiments. ***$P < 0.001$, FBS-free vs. plus 0.5% BSA; ANOVA followed by Bonferroni's test. (B) Cells grown in presence of 10% FBS were incubated, after adhesion, under different conditions (a–c) in six-well dishes for 72 h: (a) cells were incubated in presence of 10% FBS; (b) cells were incubated with 10% FBS that had been protein-depleted; (c) cells were incubated again in 10% FBS that had been protein-depleted, but supplemented with 0.5%BSA. Cell viability was assessed by the MTT assay. Data shown are means $\pm$ SEM of % inhibition of MTT-reducing activity calculated from three independent experiments. ###$P < 0.001$ protein-depleted serum [b] vs. 10% FBS [a] and protein-depleted serum plus 0.5% BSA [c]; $$$P < 0.01$ protein-depleted serum plus 0.5% BSA [c] vs. 10% FBS [a]; ANOVA followed by Bonferroni's test. (C) Cells were grown in 10% FBS in six-well dishes. After adhesion, cells were serum-deprived for 16 h and then treated with compounds for 24 h. Cell viability was assessed by the MTT assay. Data shown are means $\pm$ SEM of % inhibition of MTT-reducing activity calculated from three independent experiments.
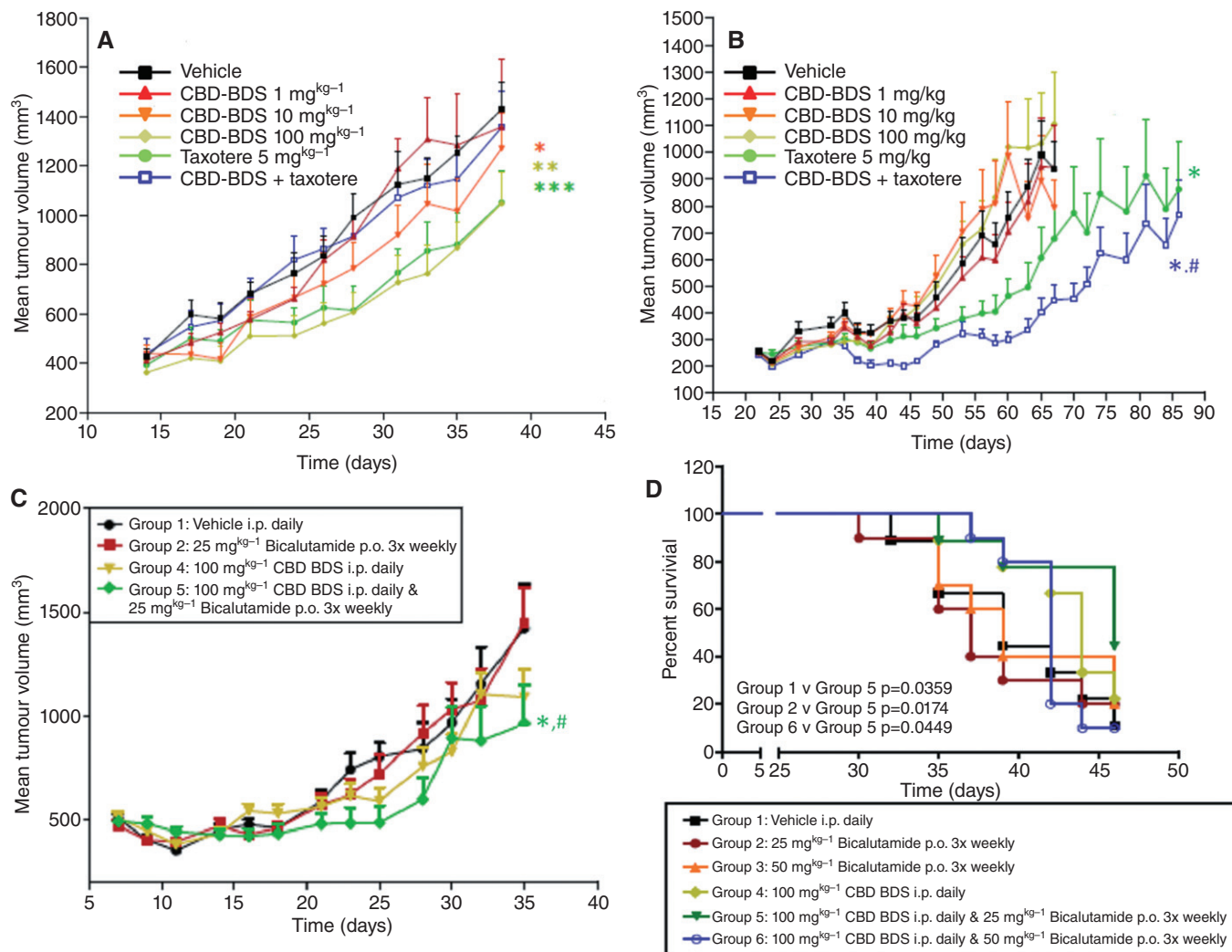
Figure 2

Effect of CBD-BDS on the growth of xenograft tumours from LNCaP and DU-145 cells in athymic mice, *per se* or co-administered with docetaxel (taxotere) or bicalutamide. Effect of increasing doses of CBD-BDS (i.p.) or docetaxel (i.v.) or combinations thereof on the growth of LNCaP (A) and DU-145 (B) cell xenografts. $N = 10$ mice were used for each group. In panel A, $*P = 0.0008$, $**P < 0.0001$ versus vehicle; $***P < 0.0001$ versus both vehicle and CBD–BDS + docetaxel; in panel B, $*P < 0.0001$ versus vehicle; $\#P < 0.0001$ versus docetaxel alone; two-way ANOVA. (C) Effect of increasing doses of CBD-BDS (i.p.) or bicalutamide (p.o.) or in combination, on the growth of LNCaP cell xenografts. A higher dose of bicalutamide (50 mg·kg^{-1}) was studied, but the effect was not different from that of the 25 mg·kg^{-1} dose. $*P = 0.0005$ (group 5 vs. group 1); $\#P = 0.001$ (group 5 vs. group 2); two-way ANOVA. (D) Kaplan–Meier survival plots for the study described in (C). Statistical significance was assessed by the Log rank-Wilcoxon analysis.

47 days of treatment, CBD–BDS plus bicalutamide significantly prolonged survival as compared with bicalutamide or CBD–BDS alone (Figure 2D).

Effect of cannabinoids on PCC caspase 3/7 activity

When the cannabinoids or corresponding BDS were tested in LNCaP cells in the presence of serum for 24 h, very little effect was observed on caspase 3/7 activity, and only with CBD (10 μM) and CBC (10 μM) (Figure 3A). In DU-145 cells, only THCV, THCVA and CBGV produced a small effect (Figure 3B). In contrast, the positive control, consisting of anti-Fas antibody plus camptothecin for 24 h, produced a strong effect in

both cell lines (Figure 3A,B). In LNCaP cells, the TRPM8 channel antagonist, OMDM233 (1 μM), exerted an effect similar to that of CBD, and the TRPM8 agonist icilin, at a dose producing no effect *per se* (0.05 μM), antagonized the effect of CBD (Figure 3A). Several BDS were more effective on caspase 3/7 activity in both LNCaP and DU-145 cells (Figure S4A,B).

When LNCaP cells were cultured under varying conditions of serum deprivation (SDP), the effect of CBD on caspase 3/7 activity was dramatically greater, whereas that of OMDM233 was reduced (Figure 3C). Also, CBC and CBG released caspase 3/7 under these conditions, although only at 20 μM in the case of CBG (Figure 3D). The extent of the effect of 10 μM CBD varied with the time of incubation or the
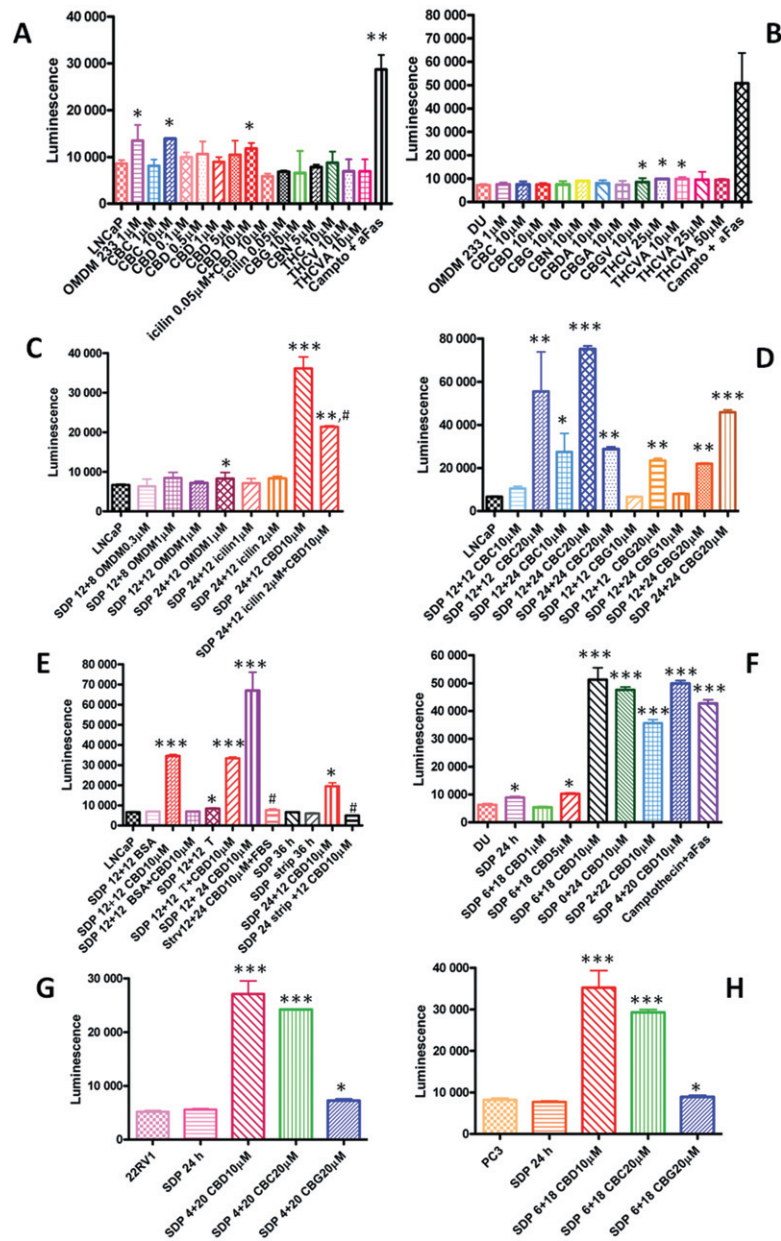
Figure 3

Effect of cannabinoids and on the release of caspase 3/7 from various PCC lines. Cells (10 000 per data point) were treated under the conditions shown, and caspase 3/7 activity was assessed with the luminescence assay. Other compounds tested that exhibited no activity are not shown. Effect of various compounds, at various concentrations, in LNCaP (A) and DU-145 (DU) (B) cells incubated in the presence of serum for 24 h, and of the positive control, anti-FAS + camptothecin (campto + AFAS). Note how the TRPM8 channel antagonist OMDM233 stimulates caspase 3/7 activity and how the TRPM8 channel agonist icilin inhibits the effect of CBD in LNCaP cells. (C) Effect of varying duration of SDP before and after treatment (12 h + 8 h treatment, 12 h + 12 h treatment, 24 h + 12 h treatment) with varying doses of the TRPM8 antagonist OMDM233, or of the TRPM8 agonist icilin, or of CBD, with and without icilin, on caspase 3/7 activity in LNCaP cells. (D) Effect of various durations of SDP before and after treatment (12 h + 12 h treatment, 12 h + 24 h of treatment or 24 h + 12 h treatment) with varying doses of CBG and CBC on caspase 3/7 activity in LNCaP cells. (E) Effect of BSA (0.5%), or testosterone (T, 50 μM), or subsequent addition of FBS, or of the use of charcoal-stripped FBS (strip) on the effect of CBD on caspase 3/7 activity in LNCaP cells. These experiments were carried out under different conditions of pre-treatment serum deprivation (12 or 24 h), whereas the treatment with CBD (10 μM) was always carried out for 12 h, thus leading to total durations of experiments of 24 or 36 h. (F) Effect of CBD on caspase 3/7 activity in SDP DU-145 cells. Experiments were carried out with either varying doses of CBD for 18 h, after a previous serum deprivation of 6 h, or with 10 μM CBD for a total of 24 h with different combinations of previous serum deprivation (0, 2 and 4 h) and treatment (24, 22 and 20 h). Finally, the effect of CBC and CBG were studied in 22RV1 (G) and PC3 (H) cells. In both cases, the experiment lasted for 24 h, with a previous serum deprivation of 4 h in panel G and 6 h in panel H. Data are means ± SEM of at least $n = 3$ experiments. Means were compared by ANOVA followed by Bonferroni's test. *$P < 0.05$, **$P < 0.01$, ***$P < 0.001$ versus respective control (first bar in each panel, which represents the baseline level of caspase 3/7, which, for a given cell line, did not vary significantly regardless of the duration of the experiment and the presence of serum in the 12–36 h range). In panels C and E, #$P < 0.01$ versus SDP 24 + 12 CBD 10 μM.

duration of serum deprivation before incubation with the compound (Figure S5). As described above for the MTT assay, only in the absence of proteins in the serum did CBD exhibit high efficacy at stimulating caspase 3/7 activity in LNCaP cells, whereas the presence or absence of testosterone (as in normal serum or charcoal-stripped serum, respectively) did not influence its effect (Figure 3E). Finally, under conditions of serum deprivation, the effect of CBD was still significantly attenuated by icilin (Figure 3C), but not by TRPV1 channel or CB_1 and CB_2 receptor antagonists [iodo-resiniferatoxin (0.2 µM), SR141716 (0.5 µM) or SR144528 (0.5 µM) respectively] (Figure S6).

CBD (10 µM) was also efficacious at elevating caspase 3/7 activity in DU-145 cells under varying conditions of SDP (Figure 3F), but CBC and CBG (20 µM) were much less active, or inactive, in these cells also under these conditions (Figure S7). Agonists of TRPV1 (capsaicin 1 µM), TRPV2 (THCV 20 µM) (De Petrocellis et al., 2011) and TRPA1 (allylisothiocyanate 100 µM) channels, which are highly expressed in these cells (Figure S1), were either inactive or, when active (as in the case of allylisothiocyanate), the effect was not antagonized by the respective antagonist (AP18, 30 µM) (data not shown).

In serum-deprived 22RV1 cells (Figure 3G) and PC-3 cells (Figure 3H), both CBD (10 µM) and CBC (20 µM), but much less so CBG (20 µM), caused marked activation of capsase 3/7 (Figure 3G,H). In the former cells, the effect of CBD was not altered by the presence of testosterone (data not shown).

Effect of CBD on apoptosis as assessed by TUNEL positivity

When cells incubated with vehicle or CBD (10 µM) under SDP conditions leading to optimal release of caspase 3/7 were analysed with a bioanalyser, significant TUNEL positivity was found in all PCC lines (Figure S8A–D, Table S4). This effect was confirmed by immunofluorescence in LNCaP and DU-145 cells treated with CBD (10 µM). Importantly, in LNCaP cells, TUNEL positivity was observed in both TRPM8-expressing and -non-expressing single cells, whereas TRPM8 channel-expressing cells were not always TUNEL-positive (Figure S9). Interestingly, TRPM8 channel immunoreactivity was not significantly decreased after serum deprivation, an effect which is in agreement with the results of the Western blot in Figure S1C. TRPM8 channel immunoreactivity was localized almost uniquely in the endoplasmic reticulum (ER), as it co-stained with the ER marker calnexin (Figure S9), a result which is also in agreement with previous studies (Bidaux et al., 2005; Valero et al., 2011).

Effect of CBD on PCC apoptosis and cell cycle

We carried out an analysis of the DNA fragmentation pattern induced by CBD (10 µM), under conditions that optimally stimulate caspase 3/7 activity (see above). A typical apoptotic DNA fragmentation pattern was found in LNCaP cells (Figure S10). Furthermore, using FACS scan analyses, we further established that CBD, apart from inducing apoptosis in these cells (Figure S8E), also caused apoptosis and inhibited the G1–S transition of the cell cycle in DU-145 cells (Figure S8F). These results are summarized in Tables S5 and S6. CBD also strongly elevated the expression of the cell cycle inhibitors p27^{kip}, only in AR-expressing PCCs (Figure S8G), and p21, in all PCCs (4.5×, 5×, 6× and 15× in LNCaP, 22RV1, DU-145 and PC-3 cells, respectively, data not shown).

Effect of CBD on PUMA, CHOP, AR, TRPM8 and p53 expression

CBD (10 µM), incubated with serum-deprived cells under conditions leading to optimal caspase 3/7 activation, up-regulated the transcriptional expression levels of the p53-up-regulated modulator of apoptosis (PUMA), a major modulator in intrinsic pathways of apoptosis, in all four cell lines under investigation (Figure 4A). CBD also elevated p53 protein expression in AR-expressing cells (Figure 4B) and CCAAT/enhancer binding protein (CHOP) mRNA expression in all cells (Figure 4C). In LNCaP cells, Ser^{46} phophorylation on p53 was also increased on top of the effect on protein expression (Figure 4B). Finally, CBD (10 µM) down-regulated AR mRNA in LNCaP and, to a smaller extent, 22RV1 cells (Figure 4D,E), and reduced basal and testosterone-induced TRPM8 mRNA levels in LNCaP cells (Figure 4F).

Effect of cannabinoids on intracellular calcium and ROS assays

We studied whether CBD was able to induce intracellular Ca^{2+} mobilization and production of ROS in all four PCCs. Our results indicated that CBD dose-dependently elevated intracellular Ca^{2+} in all four PCC lines in a manner often potentiated by SDP and independent of the presence of extracellular Ca^{2+} (Figure 5 and Table S7), and at concentrations similar to those necessary to induce apoptosis. Also, CBD activated ROS production only in LNCaP cells, in a manner dependent on SDP (Figure 5) and inhibited by intracellular Ca^{2+} chelation by BAPTA (data not shown). Two other compounds, CBC and CBG, raised intracellular Ca^{2+} in all four PCC lines (Table S7).

Effect of CBD on neuroendocrine-like differentiated LNCaP cells

Serum and androgen deprivation, as well as the presence of agents that potentiate PKA-mediated signalling (i.e. IBMX + db-cAMP), cause progressive phenotypic changes in LNCaP (but not 22RV1, PC-3 and DU145) cells, which start producing neuron-specific enolase (NSE) and making neurite-like structures (Bang et al., 1994; Cox et al., 1999; Marchiani et al., 2010). We confirmed that, similar to prolonged (72 h) SDP, 36 h incubation of these cells with IBMX + db-cAMP in the absence of serum was sufficient to induce a neuroendocrine-like phenotype (Figure S11) and an over-expression of NSE (Figure 6B). CBD (10 µM) caused a greater activation of caspase 3/7 in serum-deprived, IBMX + dbcAMP-treated LNCaP cells compared with vehicle-treated cells (Figure 6A). The effect was not significantly antagonized by icilin, nor mimicked by the TRPM8 channel antagonist, OMDM233 (Figure 6A), and was accompanied by a down-regulation of NSE mRNA (Figure 6B), and an up-regulation of PUMA and p27^{kip} mRNA (Figure 6C,D). CBD plus IBMX + db-cAMP also caused stronger down-regulation of AR and TRPM8 than those induced by serum deprivation with or without IBMX + db-cAMP alone (Figures 6E,F and 4).
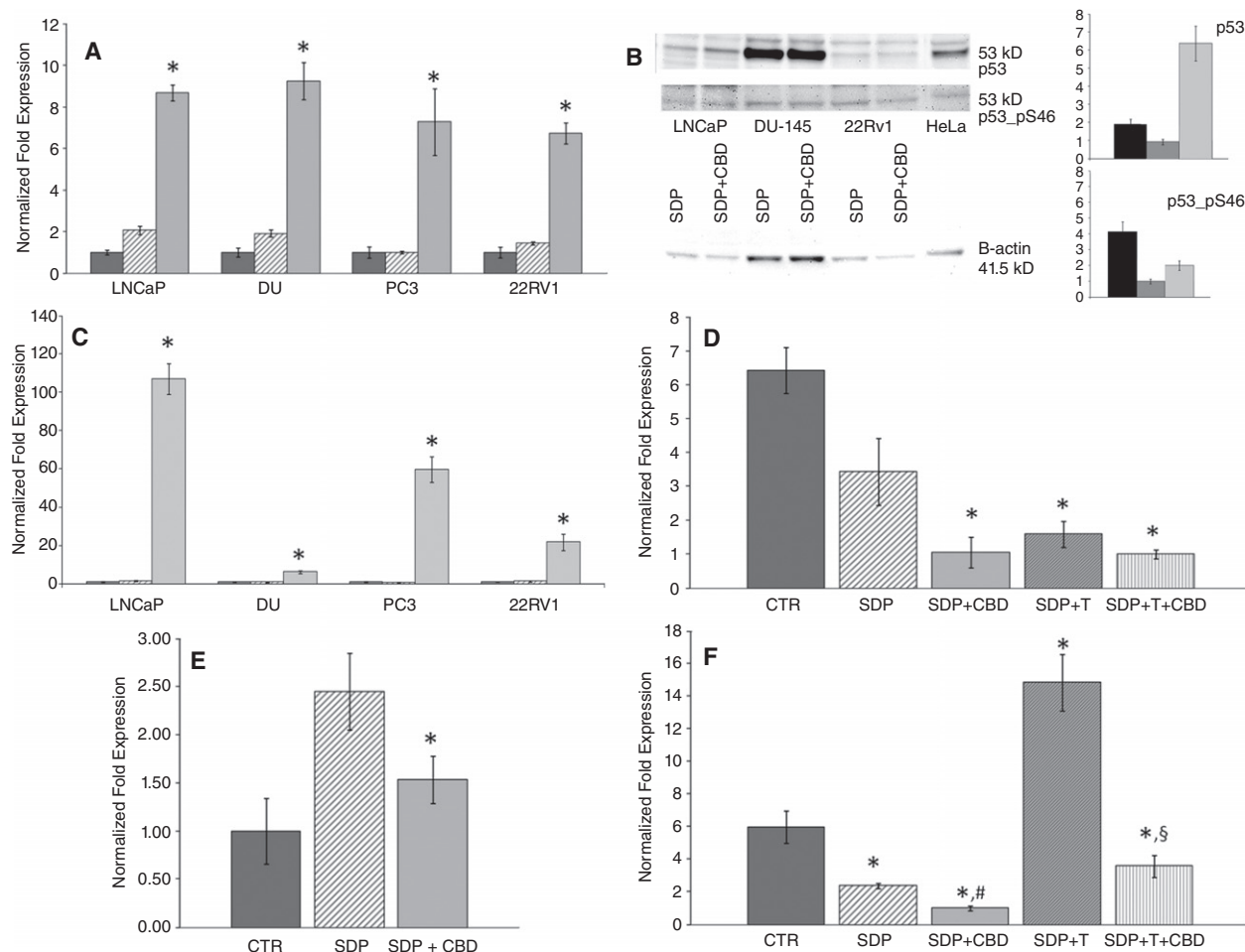
Figure 4

Molecular mechanisms of the pro-apoptotic effect of CBD in PCC lines. (A) Effect of CBD (10 µM) on the mRNA expression of the PUMA in the four cell lines examined in this study. Cells were cultured in presence of serum (dark grey bars), in serum-deprived medium for 24 h (striped bars) and in presence of 10 µM CBD in the optimal conditions evaluated by caspase 3/7 assay (light grey bars); that is, 12 h (LNCaP), 18 h (DU-145 and PC-3) and 20 h (22RV1) of CBD treatment after 12, 6 and 4 h of previous serum deprivation respectively. The expression levels, normalized respect to reference genes, were scaled for each cell line to the expression value of the cells cultured in presence of serum, put as 1. The means of the quantitative cycles (cq) for the these conditions were 28.68 (LNCaP), 28.62 (DU-145), 27.32 (PC-3) and 25.63 (22RV1). The reaction background was 37.30 cq. (B) Representative Western blots for the stimulatory effect of CBD on the expression and phosphorylation of p53 in LNCaP, DU-145 and 22RV1 cells, serum-deprived for 12 h and then treated with vehicle or CBD (10 µM) for a further 12 h. Histograms show the quantitative determination of the chemoluminescence in Western blots from two separate experiments, normalized to β-actin and expressed as fold amounts relative to the corresponding serum-deprived, vehicle-treated control cells: LNCaP (black bars), 22RV1 (dark grey bars) and DU-145 (light grey bars) cells. (C) Transcriptional expression of CHOP in prostatic cell lines: CHOP mRNA levels in LNCaP, DU-145, PC3 and 22RV1 prostatic cancer cell lines. Cells were cultured in presence of serum (first bar in each group), in serum deprived medium for 24 h (second bar in each group) and in presence of 10 µM CBD in the optimal conditions evaluated by caspase 3/7 assay (third bar in each group) (see panel A). qRT-PCR was performed, using 20 ng of cDNA per assay. The expression levels, normalized respect to reference genes, were scaled for each cell-line to the expression value of the cells cultured in presence of serum, put as 1. The means of quantitative cycles (cq) for the these conditions were 24.88cq (LNCaP), 20.73cq (DU-145), 21,79cq (PC3) and 21,87cq (22RV1). The reaction background was 35.30 cq. Standard deviations were calculated by the gene expression module of iQ5 real-time PCR. All differences indicated in the graph with (*) were statistically significant ($P < 0.05$) as evaluated according to Pfaffl, 2010 (see Supporting information). A typical experiment (R.I.N. > 8.5) is shown. (D) Transcriptional expression of androgen receptor in LNCaP and (E) 22RV1 cells. The cells were cultured in presence of serum (CTR), in serum-deprived medium for 24 h (SDP) and in presence of 10 µM CBD for 12 (LNCaP cells) or 20 (22RV1) h during 24 h total growth in serum-deprived medium (SDP + CBD). LNCaP cells (D) were also growth for 24 h in serum-deprived medium containing testosterone 50 µM in absence (SDP + T) or in presence (SDP +T + CBD) of CBD, following the conditions described above. The expression levels normalized respect to the reference gene were scaled to the lowest expression value condition [i.e. SDP +T + CBD, 26.76 cq vs. background >40 cq for (D) and CTR, 26.76 cq vs. background >40 cq, for (E)], considered as 1. (F) Transcriptional expression levels of TRPM8 in LNCaP cells cultured in presence of serum (CTR), in serum-deprived medium for 24 h (SDP) and in the presence of 10 µM CBD for 12 h during 24 h total growth in serum-deprived 50 µM in absence (SDP + T) or in presence (SDP +T + CBD) of CBD, following the conditions described above. The expression levels normalized respect to the reference gene were scaled to the lowest expression value condition (SDP, 27.30 cq vs. background at 35.01 cq), considered as 1. In panels A, C, D, E, a representative experiment (R.I.N. > 8.5) is shown and qRT-PCR was performed as described in Methods, using 20 ng of cDNA per assay. Standard deviations were calculated by the gene expression module of iQ5 real-time PCR. All differences indicated in the graph (*) were significant ($P < 0.05$ vs. values in dark grey bars) as evaluated according to Pfaffl, 2010 (see Supporting information). In panel F, # denotes $P < 0.05$ vs. SDP, and § denotes $P < 0.05$ vs. SDP + T.
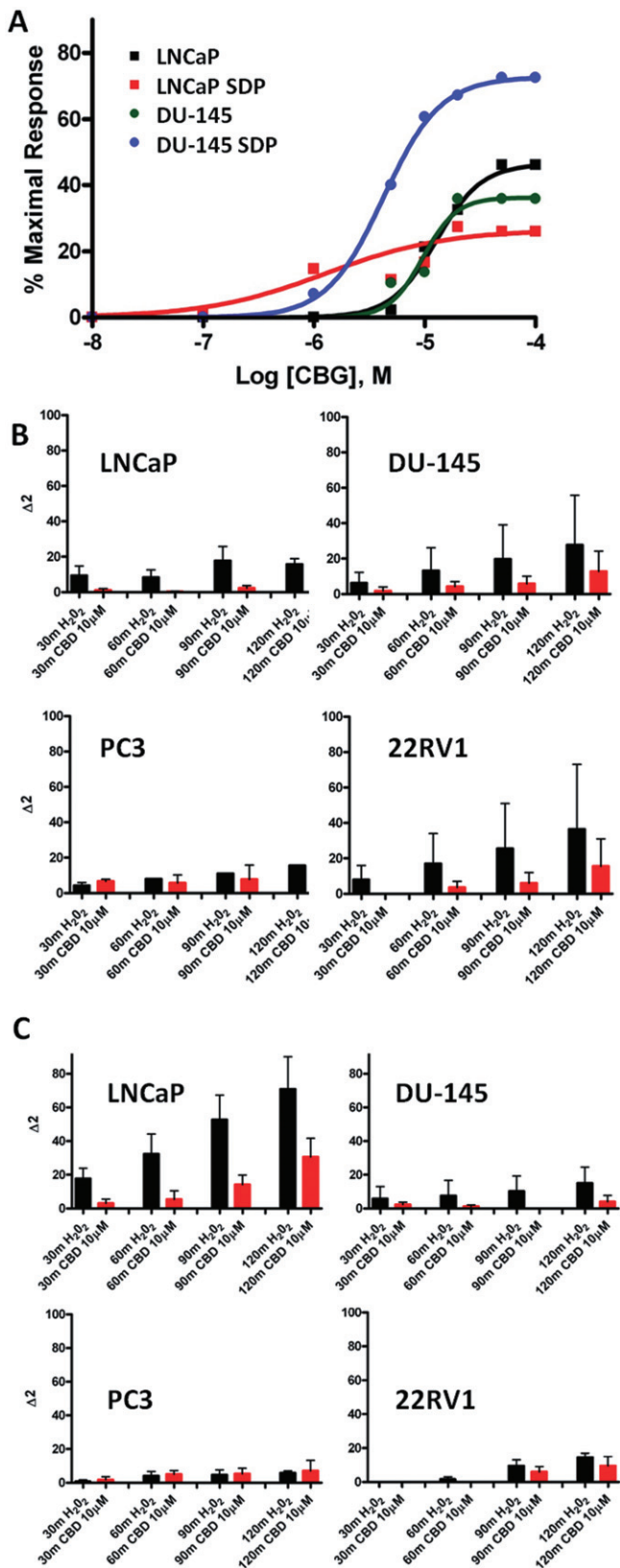
Figure 5

Effect of cannabinoids on intracellular Ca^{2+} and ROS in prostate carcinoma cells. (A) Typical dose-dependent effects for cannabinoids on intracellular Ca^{2+} in PCCs, with either efficacy or potency being higher in cells serum-deprived (SDP) for 24 h. The effect of CBG in LNCaP and DU-145 cells is shown. See Table S6 for the full data in the four PCCs with CBD, CBG and CBC. (B,C) Involvement of ROS in the effect of CBD on different PCCs. Time course of ROS production by PCC cells as measured by spectrofluorometric analysis as described in Methods. Fluorescence detection was carried out after the incubation of either 100 μM H$_2$O$_2$ or CBD (10 μM) at different times (0–30–60–120 min) in cells grown in normal medium (B) or in cells kept without serum prior to treatment (C). The fluorescence measured at time 0 was considered as basal ROS production and subtracted from the fluorescence at different times (Δ1). Data are reported as Δ2 (i.e. Δ1 values at different doses minus the Δ1 values of cells incubated with vehicle), and are mean ± SEM of at least $n = 3$ experiments. Note how the effect of both CBD and H$_2$O$_2$ becomes significant only in the absence of serum (C) and only in LNCaP cells.

Involvement of oestrogen receptors in CBD pro-apoptotic activity

The transcriptional expression levels of the oestrogen receptors, ERα and ERβ in the prostate cell lines have been extensively described in the literature (Hartel et al., 2004; Cheung et al., 2005). In particular, our data confirm in LNCaP prostate cancer cells the absence of ERα and the presence of very low (although detectable) expression levels of ERβ (Table S8). In this cell line, 17β-oestradiol did not interfere with the pro-apoptotic activity of CBD as evaluated by the caspase 3/7 assay under SDP conditions (Figure S12A). These data suggest that ERα and ERβ are not involved in pro-apoptotic activity of CBD in LNCaP cells. A high expression of G-protein-coupled oestrogen receptor 1 (GPER) was observed in all prostate cancer cell lines analysed, despite differences in the relative normalized expression (Figure S12B). Recently, G15, a high-affinity antagonist of GPER, has been identified and characterized (Dennis et al., 2009). We report that G15, at 1 μM, significantly, although not completely, attenuated the pro-apoptotic effect of CBD under SDP conditions (Figure S12C). Furthermore, G15 dose-dependently inhibited calcium release from internal stores, induced by CBD (Figure S12D).

Discussion

Non-THC cannabinoids inhibit PCC growth in vitro and in vivo

Starting from the recently described inhibitory activity of cannabinoids at TRPM8 channels (De Petrocellis et al., 2008; De Petrocellis et al. 2011) and the proposed role of this channel in determining PCC survival (Horoszewicz et al., 1983; Tsavaler et al., 2001; Henshall et al., 2003; Zhang and Barritt, 2004; Bidaux et al., 2005; 2007), we have carried out several experiments aimed at investigating the anti-cancer potential of non-THC cannabinoids and corresponding BDS in both AR-expressing and non-AR-expressing PCCs. Initially, we used the MTT assay of cell viability. The results obtained can be summarized as follows. Firstly, cannabinoids and BDS
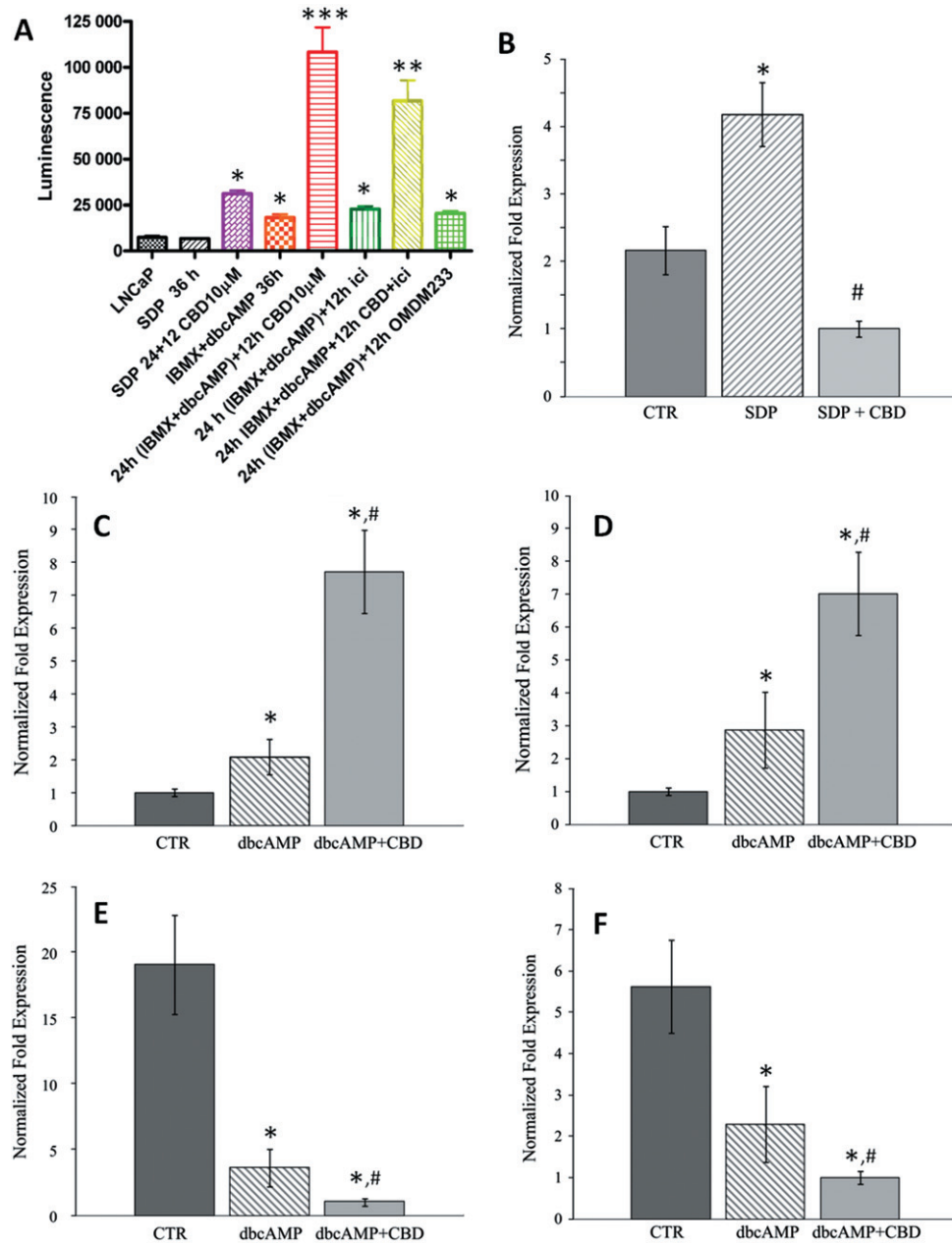
Figure 6

Effects of CBD on neuroendocrine-like LNCaP cells. Cells were differentiated with db-cAMP + IBMX for 36 h in serum-deprived medium, in the presence or absence of CBD and various other compounds. (A) Effect on caspase 3/7 activity of just serum deprivation for 36 h, alone or with CBD (10 μM) for 12 h, or with db-cAMP + IBMX for 36 h, or with db-cAMP + IBMX for 24 h followed by 12 h CBD, or with db-cAMP + IBMX followed by 12 h icilin (1 μM) or OMDM233 (2 μM), or with db-cAMP + IBMX followed by 12 h CBD + icilin. *, **, ***$P < 0.05$, 0.01, 0.001 versus SDP 36. (B) NSE mRNA in differentiated LNCaP cells. Cells were cultured in the presence of serum (CTR), in serum-deprived medium for 36 h in the presence of db-cAMP and IBMX (SDP) and in the presence of 10 μM CBD for 12 h during db-cAMP + IBMX treatment (SDP + CBD). qRT-PCR was performed using 20 ng of cDNA per assay. The expression levels of NSE mRNA, normalized respect to the reference gene, were scaled to the lowest expression value condition, considered as 1; i.e., SDP + CBD (28.67 cq vs. background >40 cq). PUMA (C), p27^{kip} (D), AR (E) and TRPM8 (F) mRNA levels in LNCaP cells following various treatments in serum-deprived (SDP) cells. Cell were cultured in presence of serum (CTR), in serum-deprived medium for 36 h in presence of db-cAMP + IBMX (dbcAMP) and in presence of 10 μM CBD for 12 h during db-cAMP + IBMX treatment (dbcAMP + CBD). For all the targets, the expression levels normalized respect to the reference gene were scaled to the lowest expression value condition, considered as 1; i.e. CTR (28.68 cq vs. background at 37.53) for PUMA and p27^{kip} (24.75 cq vs. background at 38.40cq); and db-cAMP + CBD for AR (29.04 vs. background >40 cq) and TRPM8 (29.50 vs. background at 35.80 cq). In panels B–F, qRT-PCR was performed using 20 ng of cDNA per assay, and a typical experiment (R.I.N. > 8.5) is shown. Standard deviations were calculated by the gene expression module of iQ5 real-time PCR. All differences indicated in the graph (*) were significant ($P < 0.05$) versus CTR as evaluated according to Pfaffl, 2010 (see Supporting information). # denotes $P < 0.05$ versus CTR.

reduced PCC viability with higher potency and efficacy in the absence of serum proteins, and regardless of the presence of hormones in the medium and of the androgen dependency of the PCC line under study. With serum deprivation, CBD was the most efficacious compound in three out of the four cell lines investigated. These results are in full agreement with previous observations in glioma cells (Jacobsson *et al.*, 2000). Secondly, amongst all the possible known cannabinoid targets investigated, only TRPM8 channels, when present (as in LNCaP cells), seemed to mediate, and only in part, the effect of CBD. Finally, under certain dosing conditions, CBD produced synergistic effects with docetaxel and/or bicalutamide in DU-145 and/or LNCaP cells.

Based on this first set of results, we decided to test CBD against the growth of xenograft tumours generated in athymic mice from LNCaP and DU-145 cells. As CBD–BDS was more efficacious *in vitro* than CBD in the presence of serum proteins, we administered this preparation. Given alone, CBD–BDS reduced tumour size in xenografts generated from LNCaP cells. In these tumours, CBD also significantly enhanced the anti-cancer effects of bicalutamide (extending the survival time of the animals), but not those of docetaxel. Instead, CBD–BDS was inactive by itself against the growth of DU-145 xenografts *in vivo*, although it potentiated the effect of docetaxel. These findings suggest that *Cannabis* extracts enriched in CBD might provide the basis for new therapies against prostate carcinoma, either as stand alone treatments or in addition to currently used drugs for this type of tumor.

Cellular mechanism of action of non-THC cannabinoids

We next investigated the cellular mechanisms underlying the observed effects of cannabinoids on PCCs (Table 3). As different non-THC cannabinoids might produce different effects on the cell cycle and apoptosis, leading to reduced viability in the MTT assay via different mechanisms, we focused only on those compounds that were both more efficacious in this assay and usually more abundant in *Cannabis* (i.e. CBD, CBG and CBC). The results obtained can be summarized as follows: (1) The three compounds, and CBD in particular, induced caspase 3/7 activation in all four PCC lines investigated, provided that treatments were carried out under conditions of serum deprivation. The effect was not affected by the addition of testosterone in the serum-free medium. In the presence of serum, the BDS were more efficacious than the corresponding cannabinoids. (2) CBD also inhibited the G1–S transition in DU-145 cells in FACS scan experiments, stimulated the expression of p27[kip] in AR-expressing cells and up-regulated the expression of p21 in all cells. CBD did not inhibit the cell cycle in FACS scan experiments carried out with LNCaP cells, possibly because these cells, unlike DU-145 cells, undergo a strong reduction of the G1-S phase transition during serum deprivation *per se*. The strong up-regulation of the expression of p27[kip] in these cells, as well as in 22RV1 cells, but not in DU-145 and PC-3 cells, is in agreement with previous data showing that this inhibitor of the cell cycle is more expressed in AR-expressing PCC lines, and is less important as a cell cycle regulator in non-AR-expressing cells (Galardi *et al.*, 2007).

A comparison between the results of the MTT and the caspase 3/7 activity assays allow us to make some preliminary

Table 3

Summary of the expression (mRNA expr.) of mRNA for potential cannabinoid targets and of the cellular and molecular effects of CBD observed in this study in the four prostate carcinoma cell lines under investigation

Cell line	AR mRNA expr.	CB1 receptor mRNA expr.	CB2 receptor mRNA expr.	TRPV1 channel mRNA expr.	TRPM8 channel mRNA expr.	CBD effect on cell cycle markers (p21, p27kip, G1-S phase transition)	CBD effect on apoptosis	CBD effect on PUMA expression	CBD effect on p53 phosphorylation versus expression	CBD effect on CHOP expression	CBD effect on [Ca2+]i	CBD inhibition of AR expression	Inhibitory effect of TRPM8 agonism on CBD proapoptotic action	Inhibitory effect of GPER antagonism on CBD proapoptotic action
LNCaP	+++	+	+	+	++	++	++	++	+	+++	++	++	+	+
22RV1	++	+	–	++	–	++	++	++	–	++	++	+	NA	NT
DU-145	–	–	+	++	–	++	++	++	–	+	+	NA	NA	NT
PC-3	–	+++	+++	+	+	+	+	++	p53 is not expressed	+++	++	NA	NA	NT

NA, not applicable; NT, not tested.

inferences on the cellular mechanism of action of cannabinoids, and CBD in particular. The anti-tumour effects of cannabinoids observed in the MTT assay in all PCCs appear to be due largely to stimulation of apoptosis. Accordingly, in both this assay and the caspase 3/7 assay (which is more amenable to the screening of pro-apoptotic effects than the DNA fragmentation or FACS scan analyses) we observed that the effects of cannabinoids were highest in the absence of serum, and the BDS were more efficacious than the corresponding pure compounds only in the presence of serum. There are several possible explanations for these observations. Firstly, serum deprivation causes elimination of exogenous hormones, such as testosterone, from the medium. This depletion of hormone, in turn, at least for the two AR-expressing cell lines employed here, might result in impaired survival mechanisms and/or inhibition of the cell cycle (as indeed observed for LNCaP cells), and in higher vulnerability of cells to any pro-apoptotic effects of compounds. However, we found that when LNCaP and 22RV1 cells were serum-deprived but were kept in the presence of testosterone, the efficacy of CBD at inducing caspase 3/7 activity was not reduced, nor was its effect in the MTT assay diminished. Moreover, CBD was less, and not more, efficacious when tested in LNCaP cells kept in charcoal-stripped serum, thus indicating that it is the presence of serum proteins, rather than hormones, that renders the compound less efficacious. Accordingly, addition of BSA to the serum-deprived culture medium of LNCaP cells rendered CBD inactive in both the MTT and caspase 3/7 assays. Given the high lipophilicity of cannabinoids, these observations may suggest that intracellular targets mediate their pro-apoptotic effects, and that high MW serum proteins, such as BSA, by binding to cannabinoids, prevent them from entering the cells and interacting with these targets. Indeed, past and recent evidence has demonstrated that cannabinoids bind avidly to BSA (Papa *et al.*, 1990; Fanali *et al.*, 2011). This possibility would explain why (1) also non-androgen-dependent cells were more sensitive to cannabinoids in the absence of serum; and 2) other lipophilic, non-cannabinoid *Cannabis* constituents in BDS, possibly by competing for the binding with serum proteins, increase the efficacy of cannabinoids in the presence of serum. The possibility, however, that serum deprivation, by arresting *per se* the cell cycle, as shown for LNCaP cells, predisposes cells to apoptosis independently from the absence of hormones, cannot be excluded.

Molecular mechanisms of the pro-apoptotic action of CBD

Also based on the BSA effects described above, we suggest that the pro-apoptotic effect of CBD in LNCaP cells was exerted via stimulation of intrinsic pathways of apoptosis (Table 3). This conclusion was confirmed primarily by the strong elevation of PUMA mRNA levels caused by CBD. This effect, in turn, probably follows the up-regulation of the marker of ER stress, CHOP, and the activation of p53, the two stimuli for PUMA expression. CBD also induced intracellular Ca^{2+} mobilization, another marker of ER stress, and the subsequent production of ROS, which, in these cells, might also contribute to apoptosis (Yu and Zhang, 2008). Instead, in 22RV1 cells, we observed elevation of PUMA and CHOP mRNA levels and intracellular Ca^{2+} mobilization, but no ROS elevation, nor p53 phosphorylation. Importantly, previous studies showed

that stimulation of intracellular Ca^{2+} mobilization, with or without production of ROS, is stronger in serum-deprived PCCs (Gutierrez *et al.*, 1999), and that CBD induces apoptosis in human breast cancer cells through intracellular Ca^{2+} and ROS elevation (Ligresti *et al.*, 2006; Shrivastava *et al.*, 2011), and in hepatic stellate cells via CHOP up-regulation (Lim *et al.*, 2011).

In both AR-expressing PCC lines used here, the effect of CBD was accompanied by down-regulation of AR mRNA, which might suggest that apoptosis was due, in part, to a decrease of the pro-survival effect of endogenously produced testosterone (Dillard *et al.*, 2008; Chun *et al.*, 2009). The observed up-regulation of p53 protein expression in these cells might be either the effect or the cause of AR down-regulation (Rokhlin *et al.*, 2005; Kruse and Gu, 2009; Schiewer *et al.*, 2012). The latter, in turn, is the most likely cause of TRPM8 mRNA level reduction by CBD in LNCaP cells, because TRPM8 channels are under tonic stimulation by AR in these cells (Zhang and Barritt, 2004; Bidaux *et al.*, 2005; 2007; present data). CBD-induced down-regulation of TRPM8 channels, as well as direct antagonism of these channels (De Petrocellis *et al.*, 2008; De Petrocellis *et al.* 2011), could be responsible for the pro-apoptotic effects seen in LNCaP cells (but not in 22RV1 cells, found here not to express TRPM8 channels) (Zhang and Barritt, 2004). Indeed, CBD effects were attenuated by a per se inactive concentration of a TRPM8 channel agonist. However, even in LNCaP cells other receptors must contribute to CBD pro-apoptotic effects because TRPM8 channel antagonism was not sufficient alone to produce a strong pro-apoptotic effect and CBC, which is inactive as a TRPM8 channel antagonist (De Petrocellis *et al.*, 2008; De Petrocellis *et al.* 2011), still activated caspase 3/7, whereas CBG, which is as potent as CBD at antagonizing TRPM8 channels (De Petrocellis *et al.*, 2008; De Petrocellis *et al.* 2011), was much less potent in this assay. We provide evidence that cannabinoid CB_1 and CB_2 receptors and TRPV1, TRPV2 and TRPA1 channels, which are variably expressed in the two AR-expressing cell lines employed here, do not participate in the pro-apoptotic effect of CBD. Interestingly, the effects of CBD on intracellular Ca^{2+} and ROS elevation described above are unlikely to require TRP channels and AR, as they were described previously in cells that do not necessarily express these proteins (Drysdale *et al.*, 2006; Ligresti *et al.*, 2006).

In non-AR-expressing cells, the pro-apoptotic effect of CBD was accompanied by an up-regulation of PUMA and CHOP expression and an elevation of intracellular Ca^{2+}. PC-3 cells did not express p53, an observation which is in agreement with previously reported data (van Bokhoven *et al.*, 2003). These data suggest that in these cells CBD might still act in part via ER stress and PUMA, with no involvement of AR, p53 and TRPM8 channels.

Role of adenosine and oestrogens in pro-apoptotic effects of CBD

The pharmacological profile of CBD is complex and other mechanisms might be involved in apoptotic effects. Increase in adenosine signalling is thought to be one of the mechanisms by which CBD decreases inflammation (Izzo *et al.*, 2009). In androgen-dependent and -independent human prostate cancer cells (DU-145, PC-3, and LNCaP), adenosine

was recently shown to inhibit cell proliferation by arresting cell cycle progression and inducing cell apoptosis (Aghaei et al., 2012). However, adenosine was shown to act via p53, and our data suggests that this pathway plays only a minor role in the effects of CBD, and then only in LNCaP cells. It has also been suggested that oestrogens are involved in the survival of prostate cells, and that cannabinoids may influence oestrogen metabolism (Lee et al., 2005). We analysed the role of oestrogen receptors in the pro-apoptotic effects of CBD and our data demonstrate a high expression of the G-protein-coupled oestrogen receptor, GPER, rather than ERα and ERβ, in the PCC lines used here. GPER, also known as GPR30, is an intracellular transmembrane G-protein-coupled oestrogen receptor, which resides in the endoplasmic reticulum, where it activates multiple intracellular signalling pathways (Revankar et al., 2005). 17β-oestradiol binds to GPER, resulting in intracellular calcium mobilization and synthesis of phosphatidylinositol 3,4,5-trisphosphate in the nucleus. It has been reported that activation of GPER inhibits growth of prostate cancer cells via up-regulation of p21, and induction of G2 cell-cycle arrest (Chan et al., 2010, Ren and Wu, 2012). In order to evaluate the involvement of GPER in CBD pro-apoptotic effects, a specific antagonist for this receptor, G15, which shows little affinity for ERα or ERβ at concentrations up to 10 μM, was used. Our data show that G15 was able to attenuate both CBD activation of caspase 3/7 and CBD-induced calcium release from intracellular stores in LNCaP cells, suggesting that GPER, rather than oestrogen metabolic enzymes (Lee et al., 2005) or ERα or ERβ (see also Ruh et al., 1997), may be one of the intracellular targets through which CBD stimulates the ER branch of the intrinsic pro-apoptotic pathway.

Effect of CBD on differentiated, non-AR-expressing, neuroendocrine-like LNCaP cells

Prolonged androgen deprivation and/or activation of the PKA cascade causes in some AR-expressing cells a neuroendocrine differentiation, consisting of the appearance of neurite-like structures and NSE in culture, and higher metastatic potential in vivo. This process was suggested to underlie, in part, the phenomenon by which chronic chemical castration, although efficacious at combating prostate carcinoma at its onset, results in the late formation of AR antagonist-unresponsive and highly metastatic forms of the tumour (Bang et al., 1994; Cox et al., 1999; Marchiani et al., 2010). Of the four PCC lines investigated here, only LNCaP cells were previously shown to undergo this process (Marchiani et al., 2010). We found that neuroendocrine-like LNCaP cells become more sensitive to CBD in terms of caspase 3/7 activation and PUMA overexpression, despite the fact that they exhibited strongly reduced levels of AR and TRPM8 mRNA. The pro-apoptotic effect of CBD was no longer significantly attenuated by a TRPM8 channel agonist. CBD also appeared to reverse the neuroendocrine differentiation process of these cells, as it reduced NSE expression, whilst causing further AR reduction. Thus, although antagonism of TRPM8 channels might underlie, in part, the pro-apoptotic action of CBD in non-differentiated LNCaP cells, this cannabinoid still induces the apoptosis of these cells when they become differentiated,

possibly through other non-TRPM8 mechanisms of action discussed above.

In conclusion, the in vitro data presented here allow us to suggest that non-THC cannabinoids, and CBD in particular, retard proliferation and cause apoptosis of PCC via a combination of cannabinoid receptor-independent, cellular and molecular mechanisms. Our data, however, do not argue against the previously suggested role of CB₁ and CB₂ receptors in prostate carcinoma (Sarfaraz et al., 2005; Olea-Herrero et al., 2009), although they do exclude the participation of these receptors in the effects of non-THC cannabinoids. Indeed, the effects reported here, together with previously reported cannabinoid receptor-mediated effects of THC on PCCs, might encourage clinical studies on cannabinoids and Cannabis extracts as a therapy for human prostate carcinoma, either as single agent or in combination with existing compounds. Our additional observation that differentiation of an 'androgen-dependent' cell into a more malignant and 'androgen-unresponsive' phenotype increases its sensitivity to the pro-apoptotic effect of CBD might provide a new strategy to deal with the frequent loss of efficacy of AR antagonists against prostate carcinoma growth seen after only a few years of treatment.

Acknowledgements

Conflict of interests

CGS is an employee of GW Pharma. VD is the recipient of a research grant from GW Pharma and a consultant for GW Pharma.

References

Aghaei M, Karami-Tehrani F, Panjehpour M, Salami S, Fallahian F (2012). Adenosine induces cell-cycle arrest and apoptosis in androgen-dependent and -independent prostate cancer cell lines, LNcap-FGC-10, DU-145, and PC3. Prostate 72: 361–375.

Alexander SP, Mathie A, Peters JA (2011). Guide to Receptors and Channels (GRAC), 5th edition. Br J Pharmacol 164: S1–324.

Aviello G, Romano B, Borrelli F, Capasso R, Gallo L, Piscitelli F et al. (2012). Chemopreventive effect of the non-psychotropic phytocannabinoid cannabidiol on experimental colon cancer. J Mol Med (Berl) 90: 925–933.

Bab I (2011). Themed issue on cannabinoids in biology and medicine. Br J Pharmacol 163: 1327–1328.

Bahnson R (2007). Androgen deprivation therapy for prostate cancer. J Urol 178: 1148.

Bang YJ, Pirnia F, Fang WG, Kang WK, Sartor O, Whitesell L *et al.* (1994). Terminal neuroendocrine differentiation of human prostate carcinoma cells in response to increased intracellular cyclic AMP. Proc Natl Acad Sci U S A 91: 5330–5334.

Bidaux G, Roudbaraki M, Merle C, Crepin A, Delcourt P, Slomianny C *et al.* (2005). Evidence for specific TRPM8 expression in human prostate secretory epithelial cells: functional androgen receptor requirement. Endocr Relat Cancer 12: 367–382.

Bidaux G, Flourakis M, Thebault S, Zholos A, Beck B, Gkika D *et al.* (2007). Prostate cell differentiation status determines transient receptor potential melastatin member 8 channel subcellular localization and function. J Clin Invest 117: 1647–1657.

Bifulco M, Laezza C, Portella G, Vitale M, Orlando P, De Petrocellis L *et al.* (2001). Control by the endogenous cannabinoid system of ras oncogene-dependent tumor growth. FASEB J 15: 2745–2747.

Bisogno T, Hanus L, De Petrocellis L, Tchilibon S, Ponde DE, Brandi I *et al.* (2001). Molecular targets for cannabidiol and its synthetic analogues: effect on vanilloid VR1 receptors and on the cellular uptake and enzymatic hydrolysis of anandamide. Br J Pharmacol 134: 845–852.

Blázquez C, Casanova ML, Planas A, Gomez Del Pulgar T, Villanueva C, Fernandez-Acenero MJ *et al.* (2003). Inhibition of tumor angiogenesis by cannabinoids. FASEB J 17: 529–531.

van Bokhoven A, Varella-Garcia M, Korch C, Johannes WU, Smith EE, Miller HL *et al.* (2003). Molecular characterization of human prostate carcinoma cell lines. Prostate 57: 205–225.

Caffarel MM, Andradas C, Mira E, Perez-Gomez E, Cerutti C, Moreno-Bueno G *et al.* (2010). Cannabinoids reduce ErbB2-driven breast cancer progression through Akt inhibition. Mol Cancer 9: 196–206.

Casanova ML, Blazquez C, Martinez-Palacio J, Villanueva C, Fernandez-Acenero MJ, Huffman JW *et al.* (2003). Inhibition of skin tumor growth and angiogenesis in vivo by activation of cannabinoid receptors. J Clin Invest 111: 43–50.

Chan QK, Lam HM, Ng CF, Lee AY, Chan ES, Ng HK *et al.* (2010). Activation of GPR30 inhibits the growth of prostate cancer cells through sustained activation of Erk1/2, c-jun/c-fos-dependent upregulation of p21, and induction of G(2) cell-cycle arrest. Cell Death Differ 17: 1511–1523.

Cheung CP, Yu S, Wong KB, Chan LW, Lai FM, Wang X *et al.* (2005). Expression and functional study of estrogen receptor-related receptors in human prostatic cells and tissues. J Clin Endocrinol Metab 90: 1830–1844.

Chun JY, Nadiminty N, Dutt S, Lou W, Yang JC, Kung HJ *et al.* (2009). Interleukin-6 regulates androgen synthesis in prostate cancer cells. Clin Cancer Res 15: 4815–4822.

Contassot E, Tenan M, Schnuriger V, Pelte MF, Dietrich PY (2004). Arachidonyl ethanolamide induces apoptosis of uterine cervix cancer cells via aberrantly expressed vanilloid receptor-1. Gynecol Oncol 93: 182–188.

Cox ME, Deeble PD, Lakhani S, Parsons SJ (1999). Acquisition of neuroendocrine characteristics by prostate tumor cells is reversible: implications for prostate cancer progression. Cancer Res 59: 3821–3830.

Czifra G, Varga A, Nyeste K, Marincsak R, Toth BI, Kovacs I *et al.* (2009). Increased expression of cannabinoid receptor-1 and transient receptor potential vanilloid-1 in human prostate carcinoma. J Cancer Res Clin Oncol 135: 507–514.

De Petrocellis L, Melck D, Palmisano A, Bisogno T, Laezza C, Bifulco M *et al.* (1998). The endogenous cannabinoid anandamide inhibits human breast cancer cell proliferation. Proc Natl Acad Sci U S A 95: 8375–8380.

De Petrocellis L, Vellani V, Schiano-Moriello A, Marini P, Magherini PC, Orlando P *et al.* (2008). Plant derived cannabinoids modulate the activity of transient receptor potential channels of ankyrin type-1 and melastatin type-8. J Pharmacol Exp Ther 325: 1007–1015.

De Petrocellis L, Ligresti A, Schiano Moriello A, Allarà M, Bisogno T, Petrosino S *et al.* (2011). Effects of cannabinoids and cannabinoid-enriched Cannabis extracts on TRP channels and endocannabinoid metabolic enzymes. Br J Pharmacol 163: 1479–1494.

Dennis MK, Burai R, Ramesh C, Petrie WK, Alcon SN, Nayak TK *et al.* (2009). *In vivo* effects of a GPR30 antagonist. Nat Chem Biol 5: 421–427.

Dillard PR, Lin MF, Khan SA (2008). Androgen-independent prostate cancer cells acquire the complete steroidogenic potential of synthesizing testosterone from cholesterol. Mol Cell Endocrinol 295: 115–120.

Drysdale AJ, Ryan D, Pertwee RG, Platt B (2006). Cannabidiol-induced intracellular Ca2+ elevations in hippocampal cells. Neuropharmacology 50: 621–631.

Fanali G, Cao Y, Ascenzi P, Trezza V, Rubino T, Parolaro D *et al.* (2011). Binding of Δ^9-tetrahydrocannabinol and diazepam to human serum albumin. IUBMB Life 63: 446–451.

Galal AM, Slade D, Gul W, El-Alfy AT, Ferreira D, Elsohly MA (2009). Naturally occurring and related synthetic cannabinoids and their potential therapeutic applications. Recent Pat CNS Drug Discov 4: 112–136.

Galardi S, Mercatelli N, Giorda E, Massalini S, Frajese GV, Ciafre SA *et al.* (2007). miR-221 and miR-222 expression affects the proliferation potential of human prostate carcinoma cell lines by targeting p27Kip1. J Biol Chem 282: 23716–23724.

Gertsch J, Pertwee RG, Di Marzo V (2010). Phytocannabinoids beyond the Cannabis plant – do they exist? Br J Pharmacol 160: 523–529.

Grimaldi P, Orlando P, Di Siena S, Lolicato F, Petrosino S, Bisogno T *et al.* (2009). The endocannabinoid system and pivotal role of the CB2 receptor in mouse spermatogenesis. Proc Natl Acad Sci U S A 106: 11131–11136.

Guindon J, Hohmann AG (2011). The endocannabinoid system and cancer: therapeutic implication. Br J Pharmacol 163: 1447–1463.

Gustafsson SB, Lindgren T, Jonsson M, Jacobsson SO (2009). Cannabinoid receptor-independent cytotoxic effects of cannabinoids in human colorectal carcinoma cells: synergism with 5-fluorouracil. Cancer Chemother Pharmacol 63: 691–701.

Gutierrez AA, Arias JM, Garcia L, Mas-Oliva J, Guerrero-Hernandez A (1999). Activation of a Ca^{2+}-permeable cation channel by two different inducers of apoptosis in a human prostatic cancer cell line. J Physiol 517: 95–107.

Hartel A, Didier A, Ulbrich SE, Wierer M, Meyer HH (2004). Characterisation of steroid receptor expression in the human prostate carcinoma cell line 22RV1 and quantification of androgen effects on mRNA regulation of prostate-specific genes. J Steroid Biochem Mol Biol 92: 187–197.

Henshall SM, Afar DE, Hiller J, Horvath LG, Quinn DI, Rasiah KK *et al.* (2003). Survival analysis of genome-wide gene expression profiles of prostate cancers identifies new prognostic targets of disease relapse. Cancer Res 63: 4196–4203.

Horoszewicz JS, Leong SS, Kawinski E, Karr JP, Rosenthal H, Chu TM et al. (1983). LNCaP model of human prostatic carcinoma. Cancer Res 43: 1809–1818.

Izzo AA, Borrelli F, Capasso R, Di Marzo V, Mechoulam R (2009). Non-psychotropic plant cannabinoids: new therapeutic opportunities from an ancient herb. Trends Pharmacol Sci 30: 515–527.

Jacobsson SO, Rongard E, Stridh M, Tiger G, Fowler CJ (2000). Serum-dependent effects of tamoxifen and cannabinoids upon C6 glioma cell viability. Biochem Pharmacol 60: 1807–1813.

Jacobsson SO, Wallin T, Fowler CJ (2001). Inhibition of rat C6 glioma cell proliferation by endogenous and synthetic cannabinoids. Relative involvement of cannabinoid and vanilloid receptors. J Pharmacol Exp Ther 299: 951–959.

Jemal A, Siegel R, Ward E, Hao Y, Xu J, Thun MJ (2009). Cancer statistics, 2009. CA Cancer J Clin 59: 225–249.

Kruse JP, Gu W (2009). Modes of p53 regulation. Cell 137: 609–622.

Lee SY, Oh SM, Lee SK, Chung KH (2005). Antiestrogenic effects of marijuana smoke condensate and cannabinoid compounds. Arch Pharm Res 28: 1365–1375.

Ligresti A, Bisogno T, Matias I, De Petrocellis L, Cascio MG, Cosenza V et al. (2003). Possible endocannabinoid control of colorectal cancer growth. Gastroenterology 125: 677–687.

Ligresti A, Moriello AS, Starowicz K, Matias I, Pisanti S, De Petrocellis L et al. (2006). Antitumor activity of plant cannabinoids with emphasis on the effect of cannabidiol on human breast carcinoma. J Pharmacol Exp Ther 318: 1375–1387.

Lim MP, Devi LA, Rozenfeld R (2011). Cannabidiol causes activated hepatic stellate cell death through a mechanism of endoplasmic reticulum stress-induced apoptosis. Cell Death Dis 2: e170.

Maccarrone M, Lorenzon T, Bari M, Melino G, Finazzi-Agrò A (2000). Anandamide induces apoptosis in human cells via vanilloid receptors: evidence for a protective role of cannabinoid receptors. J Biol Chem 275: 31938–31945.

Malagarie-Cazenave S, Olea-Herrero N, Vara D, Diaz-Laviada I (2009). Capsaicin, a component of red peppers, induces expression of androgen receptor via PI3K and MAPK pathways in prostate LNCaP cells. FEBS Lett 583: 141–147.

Malagarie-Cazenave S, Olea-Herrero N, Vara D, Morell C, Diaz-Laviada I (2011). The vanilloid capsaicin induces IL-6 secretion in prostate PC-3 cancer cells. Cytokine 54: 330–337.

Marchiani S, Tamburrino L, Nesi G, Paglierani M, Gelmini S, Orlando C et al. (2010). Androgen-responsive and -unresponsive prostate cancer cell lines respond differently to stimuli inducing neuroendocrine differentiation. Int J Androl 33: 784–793.

Massi P, Vaccani A, Ceruti S, Colombo A, Abbracchio MP, Parolaro D (2004). Antitumor effects of cannabidiol, a nonpsychoactive cannabinoid, on human glioma cell lines. J Pharmacol Exp Ther 308: 838–845.

McAllister SD, Murase R, Christian RT, Lau D, Zielinski AJ, Allison J et al. (2011). Pathways mediating the effects of cannabidiol on the reduction of breast cancer cell proliferation, invasion, and metastasis. Breast Cancer Res Treat 129: 37–47.

McGrath JC, Drummond GB, McLachlan EM, Kilkenny C, Wainwright CL (2010). Guidelines for reporting experiments involving animals: the ARRIVE guidelines. Br J Pharmacol 160: 1573–1576.

Melck D, De Petrocellis L, Orlando P, Bisogno T, Laezza C, Bifulco M et al. (2000). Suppression of nerve growth factor Trk receptors and prolactin receptors by endocannabinoids leads to inhibition of human breast and prostate cancer cell proliferation. Endocrinology 141: 118–126.

Mimeault M, Pommery N, Wattez N, Bailly C, Henichart JP (2003). Antiproliferative and apoptotic effects of anandamide in human prostatic cancer cell lines: implication of epidermal growth factor receptor downregulation and ceramide production. Prostate 56: 1–12.

Monet M, Lehen'kyi V, Gackiere F, Firlej V, Vandenberghe M, Roudbaraki M et al. (2010). Role of cationic channel TRPV2 in promoting prostate cancer migration and progression to androgen resistance. Cancer Res 70: 1225–1235.

Munson AE, Harris LS, Friedman MA, Dewey WL, Carchman RA (1975). Antineoplastic activity of cannabinoids. J Natl Cancer Inst 55: 597–602.

Nomura DK, Lombardi DP, Chang JW, Niessen S, Ward AM, Long JZ et al. (2011). Monoacylglycerol lipase exerts dual control over endocannabinoid and fatty acid pathways to support prostate cancer. Chem Biol 18: 846–856.

Olea-Herrero N, Vara D, Malagarie-Cazenave S, Diaz-Laviada I (2009). Inhibition of human tumour prostate PC-3 cell growth by cannabinoids R(+)-Methanandamide and JWH-015: involvement of CB2. Br J Cancer 101: 940–950.

Ortar G, Ligresti A, De Petrocellis L, Morera E, Di Marzo V (2003). Novel selective and metabolically stable inhibitors of anandamide cellular uptake. Biochem Pharmacol 65: 1473–1481.

Ortar G, De Petrocellis L, Morera L, Moriello AS, Orlando P, Morera E et al. (2010). (-)-Menthylamine derivatives as potent and selective antagonists of transient receptor potential melastatin type-8 (TRPM8) channels. Bioorg Med Chem Lett 20: 2729–2732.

Papa VM, Shen ML, Ou DW (1990). The effects of pH and temperature on the in vitro bindings of delta-9-tetrahydrocannabinol and other cannabinoids to bovine serum albumin. J Pharm Biomed Anal 8: 353–356.

Pfaffl MW (2010). The ongoing evolution of qPCR. Methods 50: 215–216.

Portella G, Laezza C, Laccetti P, De Petrocellis L, Di Marzo V, Bifulco M (2003). Inhibitory effects of cannabinoid CB1 receptor stimulation on tumor growth and metastatic spreading: actions on signals involved in angiogenesis and metastasis. FASEB J 17: 1771–1773.

Preet A, Ganju RK, Groopman JE (2008). Δ^9-Tetrahydrocannabinol inhibits epithelial growth factor-induced lung cancer cell migration in vitro as well as its growth and metastasis in vivo. Oncogene 27: 339–334.

Qin N, Neeper MP, Liu Y, Hutchinson TL, Lubin ML, Flores CM (2008). TRPV2 is activated by cannabidiol and mediates CGRP release in cultured rat dorsal root ganglion neurons. J Neurosci 28: 6231–6238.

Ramer R, Merkord J, Rohde H, Hinz B (2010). Cannabidiol inhibits cancer cell invasion via upregulation of tissue inhibitor of matrix metalloproteinases-1. Biochem Pharmacol 79: 955–966.

Ren J, Wu JH (2012). 17β-Estradiol rapidly activates calcium release from intracellular stores via the GPR30 pathway and MAPK phosphorylation in osteocyte-like MLO-Y4 cells. Calcif Tissue Int 90: 411–419.

Revankar CM, Cimino DF, Sklar LA, Arterburn JB, Prossnitz ER (2005). A transmembrane intracellular estrogen receptor mediates rapid cell signalling. Science 307: 1625–1630.

Robson P (2005). Human studies of cannabinoids and medicinal cannabis. Handb Exp Pharmacol 168: 719–756.

Rokhlin OW, Taghiyev AF, Guseva NV, Glover RA, Chumakov PM, Kravchenko JE *et al.* (2005). Androgen regulates apoptosis induced by TNFR family ligands via multiple signalling pathways in LNCaP. Oncogene 24: 6773–6784.

Ruh MF, Taylor JA, Howlett AC, Welshons WV (1997). Failure of cannabinoid compounds to stimulate estrogen receptors. Biochem Pharmacol 53: 35–41.

Ruiz L, Miguel A, Diaz-Laviada I (1999). Δ⁹–tetrahydrocannabinol induces apoptosis in human prostate PC-3 cells via a receptor-independent mechanism. FEBS Lett 458: 400–404.

Russo EB (2011). Taming THC: potential cannabis synergy and phytocannabinoid-terpenoid entourage effects. Br J Pharmacol 163: 1344–1364.

Sanchez C, de Ceballos ML, Gomez del Pulgar T, Rueda D, Corbacho C, Velasco G *et al.* (2001). Inhibition of glioma growth *in vivo* by selective activation of the CB(2) cannabinoid receptor. Cancer Res 61: 5784–5789.

Sanchez MG, Sanchez AM, Collado B, Malagarie-Cazenave S, Olea N, Carmena MJ *et al.* (2005). Expression of the transient receptor potential vanilloid 1 (TRPV1) in LNCaP and PC-3 prostate cancer cells and in human prostate tissue. Eur J Pharmacol 515: 20–27.

Sanchez AM, Sanchez MG, Malagarie-Cazenave S, Olea N, Diaz-Laviada I (2006). Induction of apoptosis in prostate tumor PC-3 cells and inhibition of xenograft prostate tumor growth by the vanilloid capsaicin. Apoptosis 11: 89–99.

Sarfaraz S, Afaq F, Adhami VM, Mukhtar H (2005). Cannabinoid receptor as a novel target for the treatment of prostate cancer. Cancer Res 65: 1635–1641.

Schiewer MJ, Augello MA, Knudsen KE (2012). The AR dependent cell cycle: mechanisms and cancer relevance. Mol Cell Endocrinol 352: 34–45.

Shrivastava A, Kuzontkoski PM, Groopman JE, Prasad A (2011). Cannabidiol induces programmed cell death in breast cancer cells by coordinating the cross-talk between apoptosis and autophagy. Mol Cancer Ther 10: 1161–1172.

Torres S, Lorente M, Rodriguez-Fornes F, Hernandez-Tiedra S, Salazar M, Garcia-Taboada E *et al.* (2011). A combined preclinical therapy of cannabinoids and temozolomide against glioma. Mol Cancer Ther 10: 90–103.

Tsavaler L, Shapero MH, Morkowski S, Laus R (2001). Trp-p8, a novel prostate-specific gene, is upregulated in prostate cancer and other malignancies and shares high homology with transient receptor potential calcium channel proteins. Cancer Res 61: 3760–3769.

Vaccani A, Massi P, Colombo A, Rubino T, Parolaro D (2005). Cannabidiol inhibits human glioma cell migration through a cannabinoid receptor-independent mechanism. Br J Pharmacol 144: 1032–1036.

Valero M, Morenilla-Palao C, Belmonte C, Viana F (2011). Pharmacological and functional properties of TRPM8 channels in prostate tumor cells. Pflugers Arch 461: 99–114.

Velasco L, Ruiz L, Sanchez MG, Diaz-Laviada I (2001). Δ⁹-Tetrahydrocannabinol increases nerve growth factor production by prostate PC-3 cells. Involvement of CB1 cannabinoid receptor and Raf-1. Eur J Biochem 268: 531–535.

Yu J, Zhang L (2008). PUMA, a potent killer with or without p53. Oncogene 27: S71–S83.

Zhang L, Barritt GJ (2004). Evidence that TRPM8 is an androgen-dependent Ca²⁺ channel required for the survival of prostate cancer cells. Cancer Res 64: 8365–8373.

Ziglioli F, Frattini A, Maestroni U, Dinale F, Ciufifeda M, Cortellini P (2009). Vanilloid-mediated apoptosis in prostate cancer cells through a TRPV-1 dependent and a TRPV-1-independent mechanism. Acta Biomed 80: 13–20.

Supporting information

Additional Supporting Information may be found in the online version of this article:

Figure S1 Transcriptional expression of TRP channels and cannabinoid receptors in prostatic cancer cell lines. First four panels: mRNA levels for TRPV1, TRPV2, TRPM8 and TRPA1 channels in LNCaP (black bars), DU-145 (pointed bars), PC-3 (striped bars) and 22RV1 (grey bars) cells. The means of quantitative cycles (cq) for the highest expression values were 26.25 for TRPV1 (DU-145), 31.13 for TRPV2 (DU-145), 26.22 for TRPM8 (LNCaP) and 26.50 for TRPA1 channels (DU-145). For all targets, the expression levels normalized respect to the reference gene were scaled to the lowest expression value, considered as 1. These were LNCaP for TRPV1 (31.70 cq vs. background at 37.53 cq), TRPV2 and TRPA1 (for both the targets the expression levels were coincident to background at 35.64 and 37.30 cq, respectively) and 22RV1 for TRPM8 channels (expression level close to background 33.05 vs. 34.80 cq). qRT-PCR was performed as described in Methods using 20 ng of cDNA/assay. Standard deviations were calculated by the gene expression module of iQ5 real-time PCR. A typical experiment (R.I.N. > 8.5; see Methods) is depicted for each gene. Two bottom panels: CB_1 and CB_2 receptor mRNA levels in LNCaP (black bars), DU-145 (pointed bars), PC-3 (striped bars) and 22RV1 (grey bars) cells. The means of quantitative cycles (cq) for the higher expression values were 27.53 for CB1 (PC-3) and 27.44 for CB2 (PC-3). For both targets, the expression levels normalized respect to the reference gene were scaled to the lowest expression value, considered as 1. These were DU-145 for CB_1 (expression level close to background 35.87 vs. 37.25 cq) and 22RV1 for CB_2 receptors (expression level close to background 35.34 vs. 36.9 cq). qRT-PCR was performed as described in Methods using 20 ng of cDNA/assay. Standard deviations were calculated by the gene expression module of iQ5 real-time PCR. A typical experiment (R.I.N. > 8.5; see Methods) is depicted for each gene. Gel image: Representative Western blot analysis of TRPM8 channels in LNCaP cells grown in serum-containing medium (CTR) and in medium deprived of serum for 36 h (SDP).

Figure S2 Effect of cannabinoid receptor or TRP channel agonists and antagonists on PCC viability in MTT assays. (A) After adhesion, cells were treated with compounds for 72 h (CPS, capsaicin; RTX, resinferatoxin). These effects were not antagonized by the selective TRPV1 antagonist, iodo-

resiniferatoxin (not shown). Only the effects of capsaicin 25 or 50 μM (in LNCaP and DU-145 cells, respectively) reached statistical significance ($P < 0.05$, ANOVA followed by Bonferroni's test). (B) After adhesion, cells were treated with allylisothiocyanate (MO), an agonist of TRPA1 channels, for 72 h. The effects of MO reached statistical significance ($P < 0.05$, ANOVA followed by Bonferroni's test) and were not antagonized by the two selective TRPA1 channel antagonists, HC030031 and AP18. (C) After adhesion, cells were treated with selective agonist (Icilin) and antagonist (OMDM 233) of TRPM8 channels for 72 h. Only the effects of Icilin 2 μM, and OMDM233 1 and 10 μM reached statistical significance, and only in LNCaP cells ($P < 0.05$, ANOVA followed by Bonferroni's test). (D) After adhesion, cells were treated with agonists and/or antagonists of CB receptors for 72 h [HU-210 was used at 10 μM; WIN55,212-2 (abbreviated as WIN) was used at 10 μM; SR141716A (abbreviated as SR1) was used at 0.5 μM; SR144528 (abbreviated as SR2) was used at 0.5 μM]. Only the effects of WIN and HU, with or without antagonists, reached statistical significance ($P < 0.05$, ANOVA followed by Bonferroni's test). In panels A–D, data are means ± SEM of % inhibition of MTT-reducing activity calculated from three independent experiments. Cells were treated in presence of 10% FBS in six-well dishes, but similar results were obtained in serum-deprived medium (not shown).

Figure S3 Interactions between cannabidiol and standard drugs on PCC viability in MTT assays. LNCaP (A) or DU-145 (C) cells were grown in presence of 10% FBS in six-well dishes. After adhesion, cells were treated with increasing concentrations of docetaxel (DCX or also indicated as DTX) tested both in the presence and absence of different concentrations of CBD for 72 h at the doses shown. (B) LNCaP cells were grown in presence of 10% FBS in six-well dishes. After adhesion, cells were treated with a suboptimal concentration of bicalutamide both in presence (MIX) and absence of CBD for 72 h. Dotted line indicates the algebraic sum of the effects of bicalutamide and CBD, each given alone. In panels A and B, data are reported as mean ± SEM of % inhibition of MTT-reducing activity calculated from three independent experiments.

Figure S4 Effect of cannabinoid BDS on the activity of caspase 3/7 in various PCC lines. Cells (10 000 per data point) were treated in the presence of serum for 24 h, and caspase 3/7 activity was assessed with the luminescence assay described in the Methods. Other BDS tested that exhibited no activity are not shown. Effect of various BDS, at various concentrations, in LNCaP (A) and DU-145 (B) cells. Data are means ± SEM of at least $n = 3$ experiments. Means were compared by ANOVA followed by the Bonferroni test. *$P < 0.05$ versus respective control (first bar in each panel).

Figure S5 Dose- and time-dependent effects of CBD on caspase 3/7 activity in LNCaP cells. Cells (10 000 per data point) were treated with CBD (1, 5 or 10 μM) under the conditions shown in the absence of serum (SDP), and caspase 3/7 activity was assessed with the luminescence assay described in the Methods. The number near 'SDP' refers to the hours of serum deprivation prior to incubation with CBD, which was carried out for the hours shown near 'CBD'. Data are means ± SEM of at least $n = 3$ experiments. Means were compared by ANOVA followed by the Bonferroni's test. *$P < 0.05$, **$P < 0.01$, ***$P < 0.001$ versus respective control (LNCaP, vehicle for 24 h). The control levels of caspase 3/7 did not

vary significantly regardless of the duration of the experiment in the 9–48 h range.

Figure S6 Effect of antagonists on CBD-induced activation of caspase 3/7 in LNCaP cells. Cells (10 000 per data point) were treated with CBD (10 μM) for 12 h after 24 h of SDP in the presence of absence of the CB$_1$ receptor antagonist, SR141716A (SR1, 0.5 μM), or the CB$_2$ receptor antagonist, SR144528 (SR2, 0.5 μM), or the TRPV1 channel antagonist, iodo-resiniferatoxin (I-RTX, 0.2 μM), and caspase 3/7 activity was assessed with the luminescence assay described in the Methods. Data are means ± SEM of at least $n = 3$ experiments. No statistically significant differences were observed towards serum-deprived cells incubated for 24 h with vehicle plus 12 h with CBD.

Figure S7 Effect of cannabinoids on caspase 3/7 activity in DU-145 cells. Cells (10 000 per data point) were treated with CBD (10 μM), CBC (20 μM) or CBG (20 μM) for 18 h in the absence of serum and after 8 h of serum deprivation (SDP), for a total duration of the experiment of 24 h. Data are means ± SEM of at least $n = 3$ experiments. Means were compared by ANOVA followed by the Bonferroni's test. *$P < 0.05$, **$P < 0.01$, ***$P < 0.001$ versus SDP.

Figure S8 Pro-apoptotic effects of CBD in LNCaP cells. (A–D) Pro-apoptotic effects of CBD in PCC cells, evaluated by TUNEL assay. The number of TUNEL-positive cells was evaluated by a Lab-on Chip approach using a Bioanalyzer (Agilent), as described in Methods. (A) LNCaP, (B) DU-145, (C) PC-3 and (D) 22RV1 prostate cancer cells were grown in absence of serum for 24 h (SPD, left panels). For CBD treatment, the cells were grown in SDP for 12 h (LNCaP), 6 h (DU-145 and PC-3) and 4 h (22RV1) and then treated with CBD (10 μM) for further 12 h (LNCaP), 18 h (DU-145 and PC-3) and 20 h (22RV1) in SDP (right panels). At the indicated times, vehicle was added to SDP conditions (see also Table S4 for quantitative data relative to the panels). (E, F) Evaluation of cell cycle by FACS scan analysis. LNCAP (E) and DU-145 (F) cells were cultured and treated with CBD (10 μM) as described for panels A–D. Cell cycle analysis was performed as described in Methods (see Tables S5,S6 for quantification of these analyses). (G) p27^{kip} mRNA levels in PCC cells. Cells were cultured in the presence of serum (dark grey bars), in serum-deprived medium for 24 h alone (striped bars) or in the presence of 10 μM CBD as described for panels A–D (light grey bars) (see above). The expression levels normalized to the reference gene were scaled for each cell line to the expression value of the cells cultured in SDP, considered as 1. The means of quantitative cycles (cq) for these conditions were 24.75 cq (LNCaP), 23.90 cq (DU-145), 25.91 cq (PC-3) and 24.71 cq (22RV1). The reaction background was 38.04 cq. A representative experiment (R.I.N. > 8.5; see Methods) is depicted and qRT-PCR was performed as described in Methods, using 20 ng of cDNA/assay. Standard deviations were calculated by the gene expression module of iQ5 real-time PCR. All differences indicated in the graph (*) were significant ($P < 0.05$ vs. values in dark grey bars) as evaluated according to Pfaffl (2010).

Figure S9 TUNEL and TRPM8 channel immunofluorescence in LNCaP and DU-145 cells. Representative images of differentially interference contrasted DU-145 (A,B) and LNCaP (C–F) cells. (A–E) Double staining for TRPM8 channel immunoreactivity and TUNEL labelling after serum deprivation

with or without (–S) CBD treatment in DU-145 (A,B) and LNCaP (C,D) cells. Note the expression of TRPM8 channels in LNCaP (C–E), but not in DU-145 (A,B) cells, and the increase of the number of TUNEL-positive cells in LNCaP and DU-145 cell lines after CBD treatment compared with starvation. The specificity of CBD-induced TUNEL immunofluorescence was shown in LNCaP cells incubated with the TUNEL label solution in absence of the enzyme terminal deoxynucleotidyl transferase (E). (F) Co-localization of TRPM8 channels and calnexin staining in TRPM8/Calnexin/DAPI merged image. Scale bar = 10 μm.

Figure S10 DNA fragmentation pro-apoptotic effect of CBD in LNCaP cells. Apoptotic fragmentation pattern was evaluated as described in Methods by Lab-on-chip technology. Electropherogram profiles showing a typical DNA fragmentation pattern in LNCaP cells growth in serum-deprived medium for a total of 24 h in the presence of vehicle (lower trace in panel A) or 10 μM CBD (lower trace in panel B) for 12 h. In both panels A and B, the electropherogram of a positive control (Jurkat cells treated for 4 h with anti-Fas plus camptothecin) was superimposed for a comparison. Insets: gel-like images of electrophoretic profiles of vehicle and CBD-treated cells.

Figure S11 LNCaP differentiation into neuroendocrine-like cells. Light microscope photo of LNCaP cells incubated with medium + serum for up to 72 h (upper panel, CTR), with medium without serum for 72 h (middle panel) or with dbcAMP plus IBMX for 36 h (lower panel). Note the neurite-like structures in the middle and lower panels.

Figure S12 Role of oestradiol and oestrogen receptors in the pro-apoptotic effects of cannabidiol. (A) Effect of 17β-oestradiol (10 μM), *per se* or given together with CBD (10 μM), on caspase 3/7 activity in LNCaP cells (10 000 cells per data point), treated under the conditions shown. Caspase 3/7 activity was assessed with the luminescence assay described in the Methods. (B) GPER mRNA levels in LNCaP (black bars), DU-145 (pointed bars), PC-3 (striped bars) and 22RV1 (grey bars) cells. The means of quantitative cycles (cq) for the highest expression values were 24.60 (LNCaP). For all targets, the expression levels normalized respect to the reference gene were scaled to the lowest expression value, considered as 1 (27,21 cq, DU-145). The background was >40 cq. qRT-PCR was performed as described in Methods using 20 ng of cDNA per assay. Standard deviations were calculated by the gene expression module of iQ5 real-time PCR. A typical experiment (R.I.N. > 8.5; see Methods) is illustrated. (C) Effect of the GPER antagonist, G15, on caspase 3/7 activity in LNCaP cells (10 000 cells per data point) treated under the conditions shown. (D) Calcium release from intracellular stores: dose-dependent effects of G15 on CBD 10 μM-induced Fura-2 fluorescence. Conditions are described in Table S7. In panel C, *P < 0.05 versus SDP + CBD; in panel D, *P < 0.05; **P < 0.01 versus CBD.

Table S1 Sequences of the q-PCR primers used in this study. Primer sequences and optimum annealing temperature (TaOpt) were designed as described in Methods. In parentheses, column 1, the target gene acronyms used in the text are shown.

Table S2 Effect of plant cannabinoids on the viability of human prostate carcinoma androgen receptor-negative (PC-3) cells. (A) Cells were seeded in presence of 10% FBS in

six-well Multiwell with a density of 6×10^4 cells·per well. After adhesion, cells were treated with increasing concentrations of compounds for 72 h (presence of serum was maintained during the treatments). (B) Cells were seeded in presence of 10% FBS in six-well Multiwell with a density of 6×10^4 cells·per well. After adhesion, cells were starved for 16 h and subsequently treated with increasing concentrations of compounds for 24 h (absence of serum was maintained during the treatments). Cell viability was assessed by MTT staining (see Methods). Data are reported as mean ± SD of IC_{50} values calculated from three independent experiments. In the case of IC_{50}>25 μM, the maximum inhibition observed at the highest concentration tested (25 μM) is shown.

Table S3 Effect of plant cannabinoids on the viability of human prostate carcinoma androgen receptor-positive (22RV1) cells. (A) Cells were seeded in presence of 10% FBS in six-well Multiwell with a density of 6×10^4 cells·per well. After adhesion, cells were treated with increasing concentrations of compounds for 72 h (presence of serum was maintained during the treatments). (B) Cells were seeded in presence of 10% FBS in six-well Multiwell with a density of 6×10^4 cells·per well. After adhesion, cells were starved for 16 h and subsequently treated with increasing concentrations of compounds for 24 h (absence of serum was maintained during the treatments). Cell viability was assessed by MTT staining (see Methods). Data are reported as mean ± SD of IC_{50} values calculated from three independent experiments. In the case of IC_{50}>25 μM, the maximum inhibition observed at the highest concentration tested (25 μM) is shown.

Table S4 Pro-apoptotic effects of CBD in PCC cells evaluated by TUNEL assay (Lab-on Chip approach; see also Figure S8). Quantitative data relative to Figure S8 (A–D). Data are expressed as the mean ± SD from two independent experiments. Jurkat cells, treated for 4 h with camptothecin and anti-Fas, were used as positive apoptotic control (18.5 ± 2.0 vs. 4.0 ± 1.9 for untreated control).

Table S5 Effect of CBD on LNCaP cell cycle as assessed by FACS scan. Quantitative data relative to Figure S8 (E). Population analysis (%) of LNCaP cells kept for 24 h with vehicle in a serum-containing medium, or kept for 12 h without serum plus 12 h treatment with either vehicle (SDP) or CBD, 10 μM, in serum-deprived medium (SDP + CBD). Data represent the means ± SD of two experiments.

Table S6 Effect of CBD on DU-145 cell cycle as assessed by FACS scan. Quantitative data relative to Figure S8 (F). Population analysis (%) of DU-145 cells kept for 24 h with vehicle in a serum-containing medium, or kept for 6 h without serum plus 18 h treatment with either vehicle (SDP) or CBD, 10 μM, in serum-deprived medium(SDP + CBD). Data represent the means ± SD of two experiments.

Table S7 Effect of cannabinoids on intracellular Ca^{2+} in prostatic cancer cell lines. The efficacies, as % of the maximum effect determined in each experiment with ionomycin (4 μM), and potencies, as EC_{50}, of CBD, CBC and CBG, are shown as means ± SD of three experiments, carried out either in cells grown in serum-containing medium or in cells serum-deprived for 24 h (SDP). *P < 0.05 versus the corresponding control (non-SDP data), assessed by ANOVA followed by the Bonferroni's test.

Table S8 Expression of oestrogen receptors ERα and ERβ in LNCaP cells. qRT-PCR analysis was performed as described in Methods. In LNCaP cells, ERα mRNA resulted undetectable; ERβ relative normalized mRNA expression was about 5-fold lower than mRNA expression observed in MCF7 human breast carcinoma cells, which were considered as 1 when calculating the relative quantity, and also used as positive control. *RNA polymerase II subunit (RNA pol) was used as reference gene. Cq, threshold cycles.

Table S9 Chemical composition of *Cannabis* enriched extracts used in this study. For each BDS, the percentage of the main cannabinoid content as well as of the other cannabinoids (w/w) are provided.